MH.S

SEARS FOUNDATION FOR MARINE RESEARCH
BINGHAM OCEANOGRAPHIC LABORATORY, YALE UNIVERSITY

MAY 31 1951
LIBRARY
FISH & WILDLIFE SERVICE
PACIFIC OCEANIC FISHERY
INVESTIGATIONS

JOURNAL OF MARINE RESEARCH

VOLUME IX, 1950

NUMBER 3

ISSUED DECEMBER 30, 1950, NEW HAVEN, CONN., U. S. A.

JOURNAL OF MARINE RESEARCH

PUBLISHED BY

SEARS FOUNDATION FOR MARINE RESEARCH

BINGHAM OCEANOGRAPHIC LABORATORY, YALE UNIVERSITY

BOARD OF EDITORS

Chairman: A. E. PARR
American Museum of Natural History
New York

C. O'D. ISELIN
Woods Hole Oceanographic Institution

H. U. SVERDRUP
Norsk Polarinstitutt
Oslo, Norway

DANIEL MERRIMAN
Bingham Oceanographic Laboratory

C.-G. ROSSBY
Institut für Meteorologi
Stockholm, Sweden

THOMAS G. THOMPSON
Oceanographic Laboratories
University of Washington

MANAGING EDITOR

YNGVE H. OLSEN
Bingham Oceanographic Laboratory
Yale University
New Haven, Conn.

The Journal is normally issued in three numbers per year constituting one volume, except for volume V, published in 1942–1944, and volume VI, published in 1946 and 1947. All the income derived from subscriptions is used solely to increase the volume and improve the quality of the Journal for the benefit of its subscribers and contributors.

Subscription price three dollars per volume, or one dollar per number. Sverdrup Anniversary Number (Vol. VII, No. 3) available only by purchase of complete Vol. VII at $3.00. Address all communications to the Managing Editor. See inside rear cover for Note to Authors.

SEARS FOUNDATION FOR MARINE RESEARCH
BINGHAM OCEANOGRAPHIC LABORATORY, YALE UNIVERSITY

JOURNAL OF
MARINE RESEARCH

VOLUME IX 1950 NUMBER 3

SLICKS, SURFACE FILMS AND INTERNAL WAVES[1]

By

GIFFORD EWING

Scripps Institution of Oceanography

ABSTRACT

Slicks, or calm streaks on a rippled sea, are often seen on coastal waters and lakes when the wind is light. They are formed by the ripple-damping action of a surface film of organic matter which occurs naturally on biologically productive waters. The ability of films to damp ripples varies radically with the degree of compaction of the film molecules. Such compaction may be caused by horizontally convergent flow in the water surface or by horizontal convergence of the wind stress. The characteristics of the resultant slicks vary with the agency producing compaction. One such agency, typical of summer conditions on the California Coast, is a train of long internal waves in a shallow thermocline. The periodic convergence and divergence of the horizontal component of orbital velocity associated with such waves produce alternate bands of compaction and extension in the surface film sufficient to cause visible differences in the rippling of the water by a slight breeze. The slicks are arrayed in parallel deployment over successive troughs of the internal wave and are spaced some hundreds of meters apart. Where the wave is progressive, the slicks also progress at the speed of the wave which is of the order of 25 cm/sec. The slicks are propagated as a wave of state traveling in the surface film which itself does not share the phase motion of the wave but only its local oscillations. This explanation is supported by theory, by model studies and by observations in the field. Internal wave slicks are not to be confused with the more closely spaced wind-cell slicks which predominate when the wind force is Beaufort 3 or greater.

[1] Contribution from the Scripps Institution of Oceanography, New Series No. 497.

INTRODUCTION

Description. Slicks, or calm streaks on rippled water, like those shown in Fig. 1, are commonly seen on harbor, coastal and lake waters when the wind is a slight breeze. They have been reported near California, Samoa, Australia, the Marquesas Islands, the Antarctic icepack, and occasionally in the open sea (Dietz and LaFond, 1950), in the Gulf of Panama (Forbes, 1945; Woodcock and Wyman, 1947), off the south coast of Borneo (J. D. F. Hardenberg, private communication), and in various Russian seas (Shuleikin, 1935, 1941). W. F. Royce of the U. S. Fish and Wildlife Service has photographed them over the Gulf of Maine, and B. N. Jamison on Lake Tahoe, California. At customary angles of observation, slicks appear whiter and brighter than adjacent zones of blue rippled water. From the air, looking nearly straight down into the sun's glitter on the sea, they appear as dark streaks. Viewed close at hand, they are sometimes hard to see but can be distinguished by the smooth oily appearance of wavelets and the absence of capillary crispations (Lamb, 1932; Art. 350). In the San Diego region they are observed at all seasons of the year, but in the summer months they are often strikingly distributed in parallel array, like bands of alto-cumulus "billow" clouds in the sky; the calm streaks, 10 to 50 m broad and arranged in congruent sinuous bands, are sometimes many kilometers long and are separated from one another by rippled zones about 300 m wide. In shallow water, such bands lie roughly parallel to contours of the bottom, but in deeper water they usually lie across the wind direction at various angles. They are visible only when the wind is sufficiently strong to ripple the water. On the other hand, at wind speeds greater than about 3.4 m/sec (Beaufort 3, the force required to sway small twigs and to straighten out flags), the slicks break up into a different pattern (Fig. 2) with narrower bands spaced much closer together and much shorter, their long axes always oriented nearly along the wind axis in a manner described by Langmuir (1938) and by Woodcock and Wyman (1947), who attribute the effect to wind cells. This paper is concerned only with slicks observed at wind speeds less than 3.4 m/sec, as shown in Fig. 1.

Analysis of the geometry of light reflection from the ocean, by the author and by Shuleikin (1935, 1941), has shown that the optical properties of calm streaks are due to the reduction of the average angle of reflection (attributed to flattening of the wavelets) and to the complete absence of capillary crispations as observed by Langmuir (1938).

Figure 1. A series of internal wave slicks off La Jolla Cove, October 1950.
Figure 2. Wind-cell slicks, typical of wind speeds greater than 3.4 m/sec. Photo of Klamath Lake, Oregon, in July 1949 by R. Revelle.

Wave-like Nature of the Phenomenon. Observations of an hour or more, sometimes with the aid of single exposure cinematography at spaced intervals, have frequently revealed a most remarkable property of the streaks, namely, that they move at right angles to their long axes at a regular rate of from 10 to 40 cm/sec, in the manner of long-period swell but very much more slowly (Ewing, 1950). This velocity is characteristic of internal waves known to exist in the shallow thermocline of summer. The wave-like nature of this motion is revealed by the fact that dye or paper placed ahead of an advancing slick does not move along with it but is overtaken, passed and left behind nearly in its original location, thus showing that a change in the state of the sea surface which is sufficient to calm ripples is being propagated without dependence on steady flow of the water itself.

The Surface Film. The physical medium in which a change of state occurs will be shown to be a contaminating surface film of organic composition, such as is known to inhibit the formation of ripples (Aitken, 1884; Gibson, G. E., 1944) and to damp those already formed (Pockels, 1891). Such a film, since it reduces the surface tension of water, spreads until it is one molecule thick (about 6×10^{-7} cm). If spread still further by some extraneous agency, the film breaks up, probably into discontinuous patches or islands of coherent material some millimeters in diameter; at the same time it loses its damping effect on ripples and its ability to depress the surface tension (Fig. 3, point D). If the area occupied by the over-expanded film is reduced by steady contraction, the film first begins to resist the contraction in an elastic manner (Fig. 3, point C); next it regains its ripple-damping ability and begins to reduce the surface tension; and then, as the islands fuse to form a continuous film (Fig. 3, point A) it abruptly becomes nearly as imcompressible as the same material in bulk (Devaux, 1914), since its molecules are then standing close-packed like sticks of chalk in a box (Langmuir, 1917).[2]

The Effect of Surface and Internal Waves. The discrete islands of an over-expanded film freely share the motion of water particles in the surface, and in consequence they may be crowded together to form a continuous ripple-damping film by horizontal convergence. This film may be broken up in turn if expanded by divergence. Such rhythmic convergence and divergence occur whenever a water surface is being alternately raised and lowered by a train of surface waves, and it has been shown by Hardman (1941) that, on lake water somewhat contaminated by naturally occurring organic matter, the surface tension alternately falls and rises during the passage of crests and

[2] For a general review of the properties of surface films, see Adam, 1941.

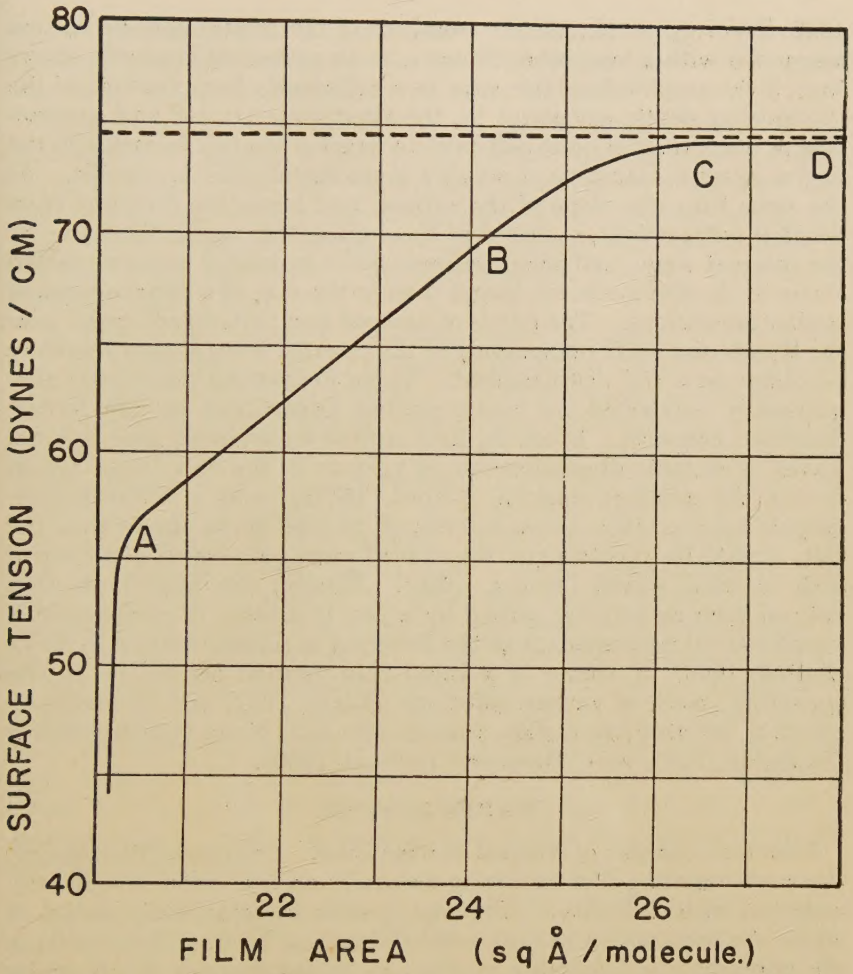

Figure 3. Variation of surface tension with degree of extension for typical film of fatty acid on water. The dashed line shows the surface tension of pure water. Redrawn from Adam, 1941.

troughs of surface gravity waves. This variation in surface tension must be accompanied by changes in the rippling, but the rapid changes of slope of the surface and the brevity of the cycle are unfavorable for the detection of such changes by visual means. On the other hand it is known that, over a long internal wave in a shallow thermocline, horizontal convergence and divergence occur throughout the upper layer over the descending and rising phases of the wave respectively (Lamb,

1932; Sverdrup, et al., 1946). Analysis of the orbital particle motion associated with a long internal wave, to be presented herewith, shows that, if the amplitude of the wave be a sufficiently large fraction of the thermocline depth, say about ¼, the alternate extension and compaction of the surface is quite sufficient to develop the full variation in the degree of ripple-damping of which a given surface film is capable. At the same time, the slope of the surface, and hence the direction from which it reflects light, is disturbed to an altogether negligible degree by the internal wave, and the durations of the expanded and compacted states of the film are much longer than in the case of a surface wave of similar dimensions. The bands of damped and undamped ripples over the trough and crest respectively of the internal wave should therefore be easily seen and distinguished. These deductions have been unequivocally supported by model studies undertaken by the writer, described herewith. Likewise, field studies have shown long internal waves of suitable dimensions to be present in the San Diego region during the summer months (Ufford, 1947a), and a bathythermographic section taken across a series of parallel slicks shows that the calm streaks lie over troughs, the rippled zones over crests, of a train of such internal waves (Ewing, 1950). Finally, the hypothesis that natural calm streaks are caused by a film in a state of compaction is supported by measurement of the lowering of surface tension in slicks (ZoBell, 1946) by means of a rapid field method dependent on the spreading power of various solutions (Adam, 1937) and by measurements of the absolute surface tension with a du Nouy type tensimeter (Shuleikin, 1935, 1941; Dietz and LaFond, 1950).

EXPERIMENTS

Chemical Analysis of Natural Marine Film. Because of its fragility, the contaminating film occurring naturally on the ocean is ordinarily collected with difficulty. However, a slick is occasionally found in which the compaction has exceeded the critical limit. This results in the crumpling and foaming of the film in the manner described by Devaux (1914) so that a narrow band of heavy scum which has lost its elasticity is formed. Samples of such scum were collected from the Scripps Institution Pier, which projects into the open sea far from any harbor. The scum was skimmed off the water into a bucket and transferred to a separatory funnel. Even the gentlest handling destabilizes some of the suspended matter, this then permitting the escape of air bubbles and throwing down the heavier solids. The solid matter was filtered out, drawn off, dried, and weighed. E. F. Corcoran of the Biochemistry Division, Scripps Institution of Oceanography, assayed the filtered and dried solids for total carbon, using

wet combustion with chromic acid (Waksman, 1936). The solid material was found to contain about 27% organic matter. No attempt was made to analyze the liquid and gaseous phases.

Contamination of the sea surface by surface-active substances of a class known commonly to have the properties on which ripple-damping depends (Adam, 1941: 50–51) strongly supports the hypothesis that calm streaks are usually due to the presence of a surface-active film and are only indirectly related to other agencies, such as variations in the flow of wind or water. This conclusion is in accord with that of Shuleikin (1935, 1941).

In view of the generally low concentration of organic matter in the sea, the high organic content of the film substance should be of interest to biologists, particularly because of reports that slicks on the ocean are sometimes zones of heavy concentration of zooplankton (Thompson, 1862; Beebe, 1926a). On the other hand, the neuston bacteria of the ocean (i. e. those depending on the surface film for support) are sometimes highly concentrated in slicks but more often show no particular relation to them (ZoBell, 1946). This variability may be due to variation in the type of slick. Those slicks associated with fairly permanent features of the water movement (for example, those formed where rivers flow into the sea) are generally distinguishable by their content of floating detritus. They probably promote production of bacteria due to the enrichment of the surface by accumulation of organic matter. On the other hand, in slicks of the type considered here, i. e. those that are the result of a traveling wave of film-compression, no such increase of productivity would be expected because the effect on the surface film is transitory. In fact, the periodic fall of surface tension might be a hazard to organisms depending on the surface for support.

Horizontal Convergence Over Internal Waves. The simplest type of internal wave (Fig. 4) is that of Stokes (Lamb, 1932; Sverdrup, et al., 1946), where it is assumed that a fluid layer of uniform density ρ' lies over a heavier layer of uniform density ρ, their respective thicknesses being h' and h. Ufford (1947b) has shown that this simple wave is a satisfactory approximation to summer conditions in the San Diego region. As with surface waves, the primary features of internal waves depend strongly on the relation of wave length to water depth, in this case to the dimensions h' and h. We shall concern ourselves only with waves long in relation to h', since internal waves of other dimensions have little effect at the upper surface. Compared to surface waves, the potential energy associated with a given deformation of the interface is much reduced due to the presence of the overlying layer,

while conversely the inertia of the system as a whole is increased. Consequently, compared to a surface wave of equal length, the velocity of propagation of an internal wave is reduced by a factor (depending on the relative densities of the two layers) which in the ocean is usually of the order of $10^{-3/2}$, i. e. about 1/30.

The streamlines and trajectories of the motion of individual water particles are shown in Fig. 4, both for a standing wave such as can be produced conveniently in a laboratory model and for a progressive wave such as is usually found in nature. The orbital particle motion

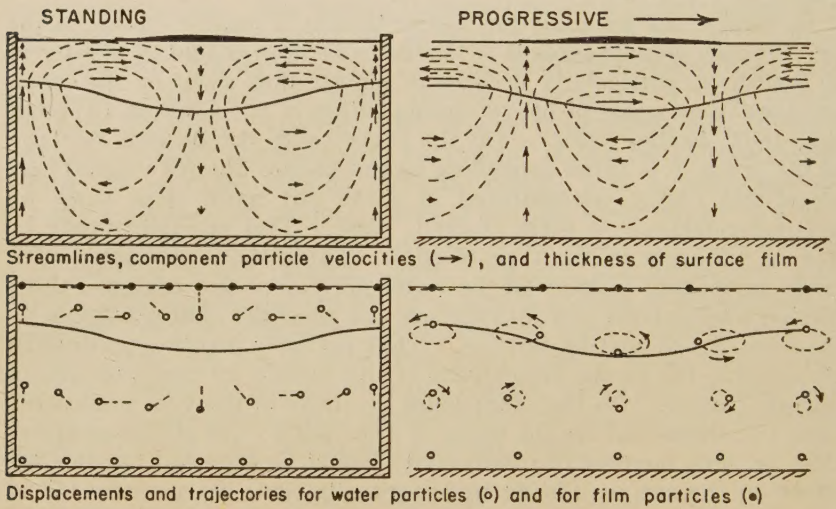
STANDING
PROGRESSIVE
Streamlines, component particle velocities (→), and thickness of surface film
Displacements and trajectories for water particles (o) and for film particles (•)

Figure 4. Long internal waves. (The extreme values of the flow and of the deformation of the interface shown together in the upper left diagram do not occur simultaneously.)

is in opposite sense in the two layers. In the upper layer the horizontal component of particle velocity, which is nearly uniform from the interface to the surface, is divergent over the rising phase of the wave and convergent over the descending phase. It can be seen by examining the distribution of surface particles in their orbits that in both types of wave the particles are most closely crowded over the trough and most dispersed over the crest of the wave. Were this superficial layer a mono-molecular film of hydrophilic substance, the condition over the trough would be one of compaction, in which ripples would be most speedily damped. If, on the other hand, the superficial film were of appreciable thickness, as in the case of a heavy coating of oil, it would be considerably thickened in this same region. As shown in Fig. 4, there is a slight vertical disturbance at the surface

which is exactly out of phase with the displacement at the interface, this displacement being required to satisfy the condition of uniform pressure along the bottom. However, the amplitude of the surface wave, which has been exaggerated in Fig. 4, is negligible in the model and in nature.

In so far as the effect on a surface film is concerned, the chief difference between standing and progressive waves is that in a standing wave the horizontal motion vanishes over the crest and trough whereas in the progressive wave it is at a maximum at these positions. Over a standing wave in a tank, a band of compaction forms alternately at the center and at the two ends of the tank. At the center, the band alternately forms by accretion from both directions during the descending phase of the wave, and then it is dispersed by scattering along each edge of the band during the rising phase. On the other hand, in the progressive wave, the zone of compaction is propagated with the same velocity as the internal wave, the zone being continuously advanced by accretion along its leading edge and scattering along its trailing edge. Over the trough, the particles are moving in the direction of wave propagation with a horizontal component of velocity

$$u' = \frac{a}{h'} c \,, \tag{1}$$

where c is the velocity of wave propagation, a the amplitude at the interface. A particle halfway between the crest and oncoming trough is at rest and is approached by the particles in motion over the trough. It is also accelerated so that by the time it is overtaken by the center of the zone of compaction it will have its maximum horizontal velocity, u', which is, however, less than c. As it is passed by the wave, it loses velocity and drops out the rear of the zone of compaction, coming to rest at a point somewhat ahead of its initial one. During the remaining half-cycle over the next wave crest it will be returned to its original position by reversal of the previous motion.

Neglecting second order terms (Lamb, 1932: Art. 228), the maximum horizontal displacement of the particles over either progressive or standing waves is given by a/kh', where k is the wave number in radians per unit of length. The amount by which the displacements from the mean positions of two neighboring particles differ is equivalent to the degree of relative extension of the surface between them, which, to the same approximation, has a/h' for its maximum value. Since the state of the surface film, and consequently its ability to damp ripples, depends on its relative compaction, a model will be similar to its prototype in this respect if the geometric similarity a/h' is preserved.

TABLE 1. KINEMATICS OF LONG INTERNAL WAVES AND EFFECT ON RIPPLE DAMPING

PARAMETER	Symbol	Unit	STANDING WAVE			PROGRESSIVE WAVE		
			FORMULA	Maximum Values in Model		FORMULA	Maximum Values Typical Ocean Wave	
				Calculated	Measured		Calculated	Measured
Potential Upper Layer Lower Layer	ϕ' ϕ		$(A \cosh ky + B \sinh ky)\cos kxe^{i\sigma t}$ $C \cosh k(y-h) \cos kxe^{i\sigma t}$			$(A \cosh ky + B \sinh ky)\, e^{i(kx-\sigma t)}$ $C \cosh k\,(y-h)\, e^{i(kx-\sigma t)}$		
Density Upper Layer Lower Layer	ρ' ρ	g/cm³ g/cm³			0.998 1.029			1.0255 1.0244
Thickness Upper Layer Lower Layer	h' h	cm cm			8 24			735 1000
Wavelength	Λ	cm			75			36,500
Wave Number	k		$2\pi/\Lambda$	.084		$2\pi/\Lambda$	.00017	
Period		sec	$2\pi/\sigma$	6.8	7.1	Λ/c	1750	1900
Frequency	σ	rad/s	(see Lamb 1932: art 231)	.941	.885	ck	.0036	.0033
Propagation Velocity	c	cm/s	σ/k	11.2	10.5	$\{g \cdot hh'/(h+h') \cdot (\rho-\rho')/\rho\}^{1/2}$	21	19
Displacement of Interface	η	cm	$a \cos kx \cos \sigma t$		2	$a \cos (kx - \sigma t)$		200
Horizontal Component of Particle Velocity	u'	cm/s	$-(a/h')c \sin kx \sin \sigma t$	2.7	4.0	$-(a/h')\, c \cos (kx - \sigma t)$	5.8	
Horizontal Displacement of Surface Particle	ξ	cm	$(a/kh') \sin kx \cos \sigma t$	3.0	3.1	$(a/kh') \sin (kx - \sigma t)$	1600	
Compaction of Surface Film			$-(a/h') \cos kx \cos \sigma t$	.25	(see Fig. 8)	$-(a/h') \cos (kx - \sigma t)$	.28	
Ripple Wavelength	λ	cm			.83	$2\pi\,(T/\rho g \cdot \Lambda/\lambda)^{1/3}$	.3	
Modulus of Decay Film Compact Film Extended	τ' τ	sec sec	$.322\,\lambda^{1.75}$ (see Fig. 5) $.712\,\lambda^2$ (see Fig. 5)	.23 .49	.23	$.322\,\lambda^{1.75}$ (see Fig. 5) $.712\,\lambda^2$ (see Fig. 5)	.040 .064	
Ratio of Moduli of Decay	τ'/τ		$.45\lambda^{-1/4}$ (See Fig. 5)	.47		$.45\,\lambda^{-1/4}$ (see Fig. 5)	.61	

The various parameters discussed above are summarized in Table I for both a standing and a progressive wave. The numerical results have to do with specific examples of a standing wave in a model and a progressive wave in the ocean which will be described presently. The analysis of Table I follows Lamb (1932: Art. 231) and Sverdrup et al. (1946: 585–589).

Ripple Damping. The precise relation between film compaction and ripple damping cannot be calculated, because there is available neither a complete theory relating damping to the state of the film nor direct empiric knowledge of changes of state with extension for a naturally occurring film.

For waves whose energy is dissipated by viscosity in the absence of interference from an elastic surface film, Stokes calculated a modulus of decay $\tau = \frac{1}{2}\nu k^2$, where ν is the kinematic viscosity and τ is defined by the relation

$$a = a_0 e^{-t/\tau}, \tag{2}$$

where a_0 is the initial amplitude and a is the amplitude at any later time t. For water, and in terms of wavelength, the numerical value of τ is given by

$$\tau = 0.712\lambda^2 \text{ seconds} \tag{3}$$

if λ, the wavelength, is expressed in centimeters (Lamb, 1932: Art 348).

Where the surface, instead of being quite free, is elastic because of contamination by a film in a critical state of extension, wave energy must be dissipated at an increased rate by the alternating tangential drag on the water as its surface is contracted and expanded by the crests and troughs of the waves (Reynolds, 1880). Lamb (1932: Art 351) attempted to "submit this explanation, to a certain extent, to the test of calculation." For wavelengths between a fraction of a millimeter and several meters, the modulus of decay, τ', is $(8/\nu k^2\sigma)^{1/2}$, where σ is the frequency in radians per second. The numerical value of τ' in seconds may be computed from the wavelength in centimeters by the following formulae:

$$\text{for capillary ripples } \tau' = 0.322\,\lambda^{1.75} \text{ seconds;} \tag{4a}$$

$$\text{for gravity waves } \tau' = 0.375\,\Lambda^{1.25} \text{ seconds.} \tag{4b}$$

For longer wavelengths viscous damping is negligible and for extremely minute ripples the calculation fails because the assumptions on which it is based are violated. Curves of τ and of τ', together with their ratio τ'/τ, are given in Fig. 5.

Reynolds' explanation (Lamb, 1895: Art 304) is based on the sup-

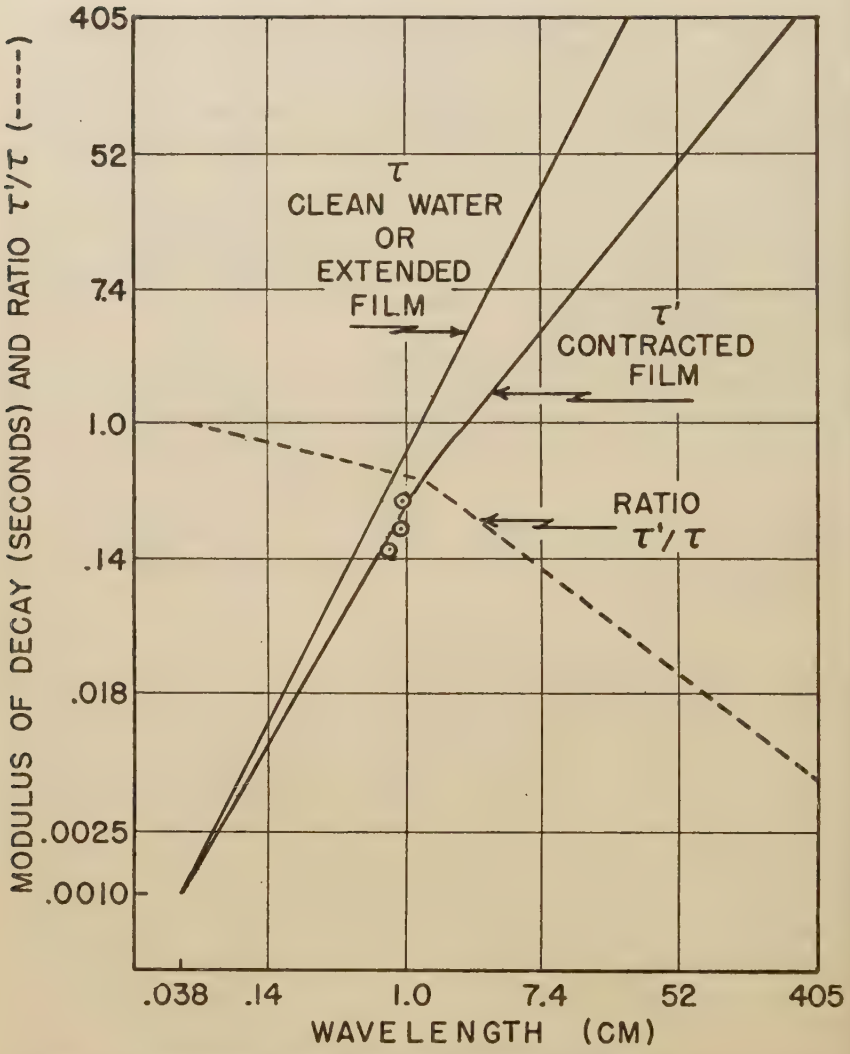

Figure 5. The modulus of decay for various wavelengths for clean water, or under an extended film (τ) and under a contracted film (τ'). The dashed line shows their ratio τ'/τ. The circled points are values observed in model experiments.

position that the surface tension varies by an amount proportional to the extension, so that

$$T = T_0\left(1 + f\frac{d\xi}{dx}\right), \tag{5}$$

where T_0 is the tension in the undisturbed state, ξ is the horizontal displacement of a surface particle, and f is a numerical coefficient proportional to the slope of the surface tension curve (Fig. 3). But, to quote Lamb, the elasticity of the film has the effect "of practically annulling the horizontal motion at the surface. The dissipation is therefore (within limits) independent of the precise value of f." Since the film is elastic only when the surface tension varies with the degree of compaction, it follows that τ applies to film states where f vanishes, that is, to the right of point C in Fig. 3. Likewise, τ' must apply where f is finite, as in the region to the left of point C, and must be constant where f is constant, that is to the left of B. It can be seen that the full range of damping rates between τ and τ' must be exhibited within a relatively narrow range of film extension corresponding to the shoulder of the curve between points B and C. This region is that in which the film loses its depressing effect on surface tension and hence its spreading tendency. Films in nature, if they are in equilibrium with the surface tension of water, must therefore tend to be nearly in a critical state of extension with regard to ripple damping.

The only previous experimental test of these equations appears to be that of Pockels (1891), who found a constant high damping rate, equivalent to τ', for films compacted beyond the point B in Fig. 3 where surface tension falls rapidly and a constant low damping rate, equivalent to τ, for films compacted to any degree less than half this amount. The damping times varied by a factor of 5.7 between these extreme conditions.

For any particular film substance, the shape of the shoulder of the curve of surface tension versus extension varies with the chemical composition and temperature of the substance and with the pH and other ion-concentrations of the underlying fluid. For the film found on the ocean, the applicable curve could be determined only by delicate laboratory methods that are not readily applied in the field (Adam, 1941: 27–35). However, the Pockels results, which are for an unspecified film-substance, are typical of a wide variety of organic compounds (Adam, 1941: 50–51). Therefore, it seems reasonable to assume that, for a film initially in equilibrium with the surface tension of water, an extension and contraction of the order of $\pm$ 25% will produce the full range of damping effect of which the film is capable, the ratio of maximum and minimum rates being, from (3) and (4a),

$$\frac{\tau'}{\tau} = 0.45\lambda^{-1/4}. \qquad (6)$$

Finally, in order to examine the ability of wind of a given speed to maintain ripples in spite of viscous damping, W. H. Munk of the

Scripps Institution has made calculations (following a method due in part to Jeffreys; see Lamb, 1932: Art 348) that show the effect for various wind speeds of a contaminating film in its extended (τ) and contracted (τ') state. His main results, kindly made available as Fig. 6, are that the minimum wind speed for growth of waves is 245 cm/sec when the surface is elastic (film compacted) compared to 110 cm/sec when the surface is free (film absent or extended). In each case the first waves to achieve stability at minimum wind velocities are gravity waves. Increased wind speeds produce a spectrum of stable waves.

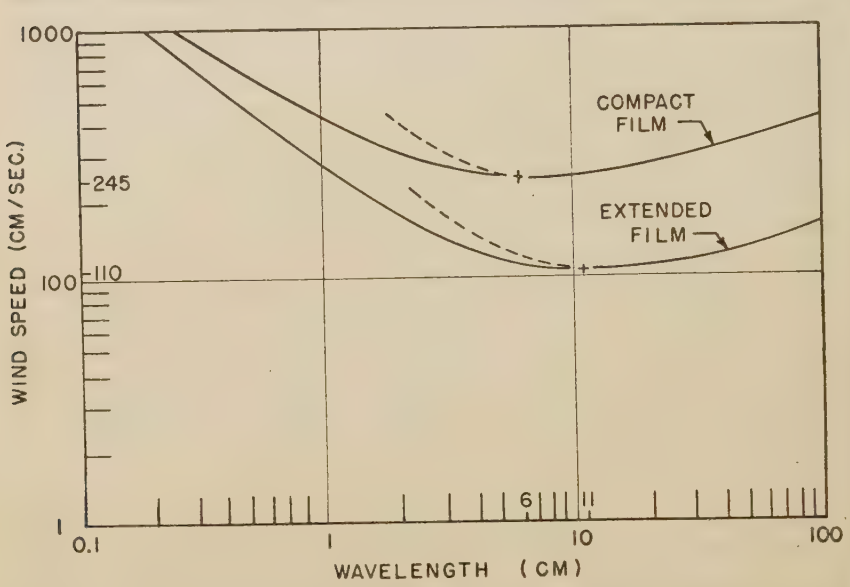

Figure 6. Limits of the spectrum of stable waves (————) and the "preferred" wave length (– – – –) for various wind speeds.

Corresponding to each wind speed, waves of a particular "preferred" length will grow fastest. The preferred wavelength is shorter at higher wind speeds.

Summary and Hypothesis. The foregoing analysis leads to the hypothesis that whenever a long internal wave exists at the interface between two layers of water with an amplitude exceeding ¼ of the thickness of the upper layer, such a wave will produce over its troughs horizontal convergence at the upper surface sufficient to bring an organic surface film into a state of compaction where ripples will be damped at the maximum rate which the film can cause; conversely, it will produce over its crests divergence sufficient to extend the film to a

state where the rate of ripple-damping is minimal. The differences in rippling will be plainly evident, whether the ripples are produced at one point by a mechanical vibrator (as in a model experiment) or uniformly over a given area by wind blowing at a speed of 110 to 340 cm/sec. If the internal wave is a standing wave, as in a model, calm zones will appear and vanish alternately over each antinodal point of the wave, the phase being opposite at adjacent antinodes, with the calm phase coinciding at each point with the depression of the interface. If the internal wave is progressive, as in nature, calm zones will remain continuously over the troughs of the wave and will themselves move as a wave of state along the surface film, their speed being governed by the propagation velocity of the internal wave.

The foregoing hypothesis has been put to the test of experiment and observation.

Model Experiments. In order to study the effect of an internal wave on a surface film, a model was set up in the laboratory. It consisted of a standard aquarium containing a layer of clear tap water over an 8% solution of cane sugar (specific gravity 1.029) which was colored red with photographic opaque. A glass plate, slightly narrower than the tank and somewhat more than one-third its length, was laid horizontally on wire supports 6.5 cm. beneath the surface of the lower layer. A synchronous motor, connected to a suitable variable speed-reduction transmission, was used to rock the glass plate through an angle of 10° about its median horizontal axis, which was transverse to the aquarium and located ¼ the length of the aquarium from one end. This gentle motion, when the period was critically adjusted, produced a standing wave with an amplitude of 2 cm (4 cm height) and a fairly sinusoidal profile. By suitable change of the period, a half-wave or a three-halves wave was easily produced. Once established, the stratification is very stable and the layers remain distinct for several days. The upper layer can be floated onto the lower one by allowing the water to drip from a separatory funnel onto a supported watch glass, or, if care be taken to make a uniform sugar solution in advance, the lower layer can be run in below the upper layer. Lacking a suitable motor to govern the wave, the glass plate could be rocked by hand, but in this case it would be better to use a less dense sugar solution so that the period would be slower and less critical. When first examined, the free surface may be found so strongly contaminated as to be nearly inextensible, that is, in the state represented in Fig. 3, to the left of point B. (The same condition is commonly observed at the surface of newly brewed China tea.) The surface is easily cleaned by floating absorbent paper upon it and removing it with a stripping motion. A light dusting of talc revealed the horizontal motion of the surface as

well as the cycles of convergence and divergence in a spectacular way, the converging particles of talc coming together with the appearance of shock at the limiting minimum area, point A in Fig. 3. Any oil of vegetable or animal origin will restore the necessary amount of contamination to the surface should it be cleaned to an unwanted degree.

A second effect of the internal wave is the periodic variation of the thickness of the superficial layer. This was studied by placing a rather heavy film of oil on the surface, which then loses its horizontal motion but exhibits interference colors that vary through the primary visible spectrum and sometimes on into the secondary one with each cycle of the internal wave, thus showing a change of thickness of some thousand Ångstrom units.

To test the effect of film compaction on ripple damping, advantage was taken of a mechanical device designed by E. A. Williams of Santa Barbara College. It consisted of a light horizontal lucite bar 15 cm long of inverted triangular section 5 mm at the base, attached by a short vertical tube to the diaphragm of a small magnetic radio speaker. The speaker was driven by an audio-oscillator through a power amplifier at frequencies that could be varied from 10 to 60 cycles/sec. The amplitude could also be controlled. With the lucite bar just touching the water surface and with the speaker driven at 36 cycles, a regular train of 8 mm ripples could easily be seen crossing the aquarium when the surface was nearly clean. They were nearly obliterated by larger amounts of contamination. In order to photograph these minute ripples, a photoflood lamp was directed at the surface so that the shape and uniformity of its reflection could be observed. In the absence of ripples, the reflection was quite round and specular. On the other hand, when ripples were present, they broke up the reflection into corrugations within an envelope which was elongated along the axis of the ripple train. Since the ripples were subject to damping during their passage across the reflection, those to the left were steeper than those to the right, thus resulting in greater elongation to the left and hence in the egg-shaped envelopes shown in Fig. 7. The rate of damping was calculated from the asymmetry of the envelope in the compact phase and it was found to be in fair agreement with the values calculated for τ' by means of equation (4a). The experimental values for three separate cycles of the internal wave are shown as circled points in Fig. 5.

The relations betweeen the internal wave, the extension of the surface, and the rippling are shown in Fig. 7, where the reduction of rippling over the trough of the internal wave is clearly evident. The relation between the calculated and the actual dimensions of the wave motion, film extension and ripple damping are entered in Table I.

Figure 7. The model in action. Columns are matched and represent a sequence of exposures at intervals of ½ wave period. Top row, particles of talc on the surface in alternate states of compaction and extension; second row, film compaction and ripple damping; third row, high and low rates of damping; bottom row, alternating phases of the internal wave.

A cine film of the surface was used to measure, frame by frame, both the extension of the film, as revealed by the separation of two arbitrarily chosen neighboring particles of talc, and the simultaneous steepness of the ripples, as revealed by the elongation of the envelope of light reflection to the left. The result is presented in Fig. 8, where the abrupt change of slope of the curves which show the separation of the particles indicates that there was a definite limit to the degree of compaction that the film would tolerate. The central curve, which shows the time variation of envelope extension, reveals that the ripples were fully damped at a compaction somewhat less than the maximum.

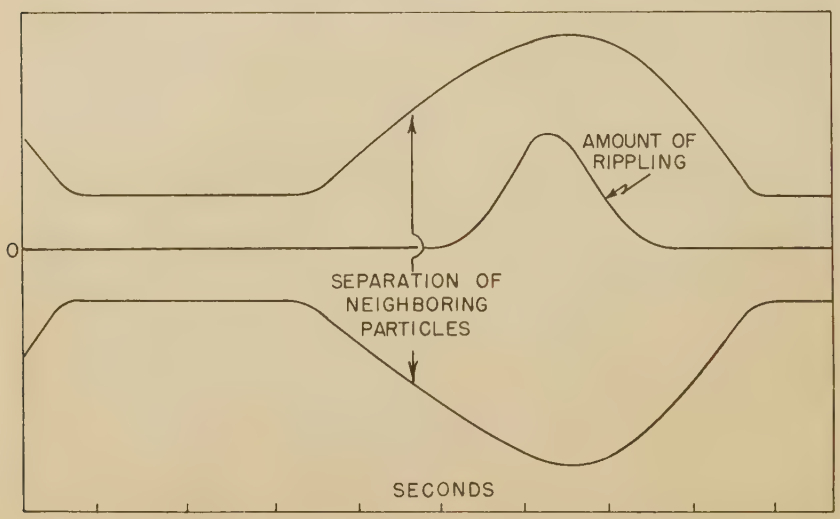

Figure 8. Extension and contraction of a surface film over a standing internal wave showing the effect of limited film compressibility and its relation to ripple damping.

This is in agreement with Pockels' results, and it shows that considerable damping effect would have been produced by an internal wave of a/h' ratio even smaller than $\frac{1}{4}$.

Finally, although it is probably implicitly clear to the reader that the transfer of the state of film compaction between adjacent antinodes of the wave was wave-like in character, yet it must be explicitly stated that such was the case. For the wave detailed in Table I, the shift of calm phase from the center to the ends of the model was over a distance of 37.5 cm, yet the maximum horizontal displacement of individual particles of the surface film was observed to be only 3.1 cm, thus proving that the ripple-damping effect was truly a change of state which was propagated independently of any but small oscilla-

tions of the medium. For reasons which will appear presently, events in nature are not favorable to such exact observation. However, it is reasonable to assume that, under similar kinematic conditions, the behavior of the sea surface is similar to that of the model surface, with the difference that, as in the ocean we expect to find progressive rather than standing internal waves so, correspondingly, we shall expect the wave of film compaction on the ocean to be propagated with a steady velocity instead of vanishing at one antinode while simultaneously appearing at the adjacent ones.

FIELD OBSERVATIONS

Long Internal Waves in the Sea. Turning now to the ocean or to large lakes to see whether internal waves have similar effects on the larger natural scale, it is easily established that the condition $a/h' \geqslant \frac{1}{4}$

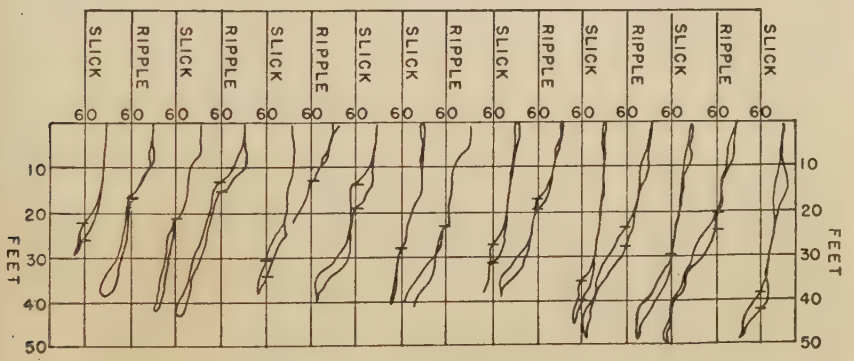

Figure 9. A series of bathythermograms taken in rapid succession from a moving ship together with simultaneous observations of slicks, showing the elevations and depressions of 60° F isotherm in relation to the presence of ripples or slicks at the sea surface.

is satisfied in the summer when the thermocline is shallow. On June 17, 1949, near San Diego, the writer used a bathythermograph (Spilhaus, 1938) to measure an internal wave with an average amplitude of 200 cm about a mean depth of 735 cm, for which the ratio a/h' is 0.27 (Fig. 9). Ufford (1947a), using a different method, measured in the same region and season (but at an unreported depth) an internal wave of 16 min period with a length of 330 m and an amplitude of 228 cm, and another of 12 min period, 130 m length and 152 cm amplitude. These were progressive waves which would produce the particle motion shown in Fig. 4. The calculated velocities associated with such a wave, together with the displacement of particles in the surface

and the resulting film compaction, are shown in Table I, where, for easy comparison, these calculations are placed alongside those for the experimental tank. It is seen that compaction, the parameter on which ripple-damping depends, is little altered in going from model to prototype. Therefore, one would expect to find parallel streaks of calm over the successive troughs of a train of such internal waves which would move along the surface at a velocity equal to the propagation velocity of the internal wave. The occurrence of such slicks was reported by the author (Ewing, 1950) and is illustrated in Fig. 1. The superficial resemblance to long-crested swell is apparent.

Bathythermograph Observations. In order to test the relation of such a series of calm streaks to internal waves, a temperature section was made, using a bathythermograph specially modified for observations shallower than 50 feet (15 m). The section was taken from a ship moving along a track normal to the long axes of the streaks and roughly at right angles to the coastline. The instrument was lowered successively in each slick and in the approximate center of each intervening rippled zone, starting with the inshore slick of the series. The resulting traces are arrayed in their proper order in Fig. 9 where, for the sake of simplicity, only the depth of the 60° F (15°.6 C) isotherm is shown. It will be seen that under each calm streak this isotherm was depressed relative to its depth under adjacent rippled zones. The alternate rise and fall of the isotherm is interpreted to correspond to the crests and troughs of a train of internal waves. The average depth of the isotherm is 24 ft (735 cm), and the average vertical displacement, corresponding to the amplitude of the wave, is ± 6.6 ft (200 cm), giving the ratio $a/h' = 0.27$, as noted above. Thus it is shown that, where natural slicks are arranged in a series of equidistant lines over a long internal wave, they are situated over the troughs of the wave, as in the model.

The Distance between Slicks. On the proposed hypothesis, the distance between the calm streaks of a series should correspond to the wavelength of the accompanying internal wave. The interslick interval of a series (which included those previously examined by bathythermograph) was measured by sailing across the slicks in the direction described above, noting the time of passage through each successive slick on the moving tape of a sonic depth recorder. Inside the 85 m contour of water depth, the slicks were fairly evenly spaced at intervals varying from 395 to 630 m with an average interval of 486 m. These may be compared as to magnitude with the wavelengths of the two internal waves measured by Ufford in July 1945, namely 330 m and 130 m.

Along the slope of a sudden declevity beyond the 85 m contour, the slicks were crowded together at an average interval of 102 m. A photograph made by W. F. Royce shows a similar terminal aggregation of streaks in one pronounced band; Forbes (1945) has reported the same distribution in Panama Bay. These may mark regions in which short period internal waves are generated. Indeed, a mechanism whereby internal waves may be generated by a tidal current running against a submerged shelf has been proposed and experimentally demonstrated by Zeilon (1934).

Propagation and Refraction. In order to see whether serially arranged calm streaks move with the velocity of propagation of progressive internal waves, studies were made with a motion picture camera by exposing film at a rate of six frames per minute. When this film is projected at 16 frames per second, the calm streaks are seen to progress sideways to their long axes, as long crested swells do. The rate of progress was found to be 22 cm/sec on May 17, 1949 and 16 cm/sec on June 13, 1949. These velocities are comparable to those measured by Ufford (1947a) for two July internal waves which were 35 and 18.5 cm/sec.

Since the propagation of long internal waves is dependent on depth according to the equation

$$c^2 = g \frac{hh'}{h+h'} \frac{\rho-\rho'}{\rho}, \qquad (7)$$

where g is the acceleration of gravity, internal waves must be refracted so as to approach parallelism to the contours of both the bottom and the thermocline (Munk and Traylor, 1947). Consequently, off the coast of San Diego, where the bottom and the thermocline gently slope away from shore, internal waves in shallow water should be oriented roughly parallel to the coast. This tendency is reflected in the orientation of slicks which parallel the shore regardless of wind direction, provided the wind is light. Where the bottom contours are sharply curved, as over a canyon, the internal waves should be convex toward shore. Correspondingly, surface streaks over La Jolla canyon have been observed to have this configuration, each one bowed congruently so that it would fit its neighbors if placed in contact.

The Reflection of Light from the Sky. The intuitive supposition that the optical effect of slicks is due to decrease in wave steepness can be rigorously examined by observing the sun's glitter path on the water. Hulburt (1934) has shown that the width of the path depends on wave steepness. Observation reveals that where a calm streak crosses the sun's path it reduces the path width to zero. Hulburt has also shown

that the light reflected by the sea, when ruffled by a 5 to 20 knot wind, is from an average altitude of 30° above the horizon. Consequently, on a clear day a rippled sea is quite blue. In slicks, however, where the wave steepness is less, the light is reflected from near the horizon, so that in contrast to the blue color of the rippled zone the calm streaks are whiter. Studies of calm streaks by Shuleikin (1935, 1941), using a somewhat different theoretical approach, yielded similar results.

Particle Motion on the Sea Surface. The hypothesis that calm streaks over internal waves are themselves propagated as waves requires that the material of the surface film shall not follow the steady phase motion of the wave but only the oscillatory horizontal particle motion. It has turned out to be difficult to observe this directly because of inability under natural conditions so to mark the film itself that its motion may be distinguished from that of water lying a few millimeters beneath and from that of objects such as bubbles having some windage profile. Close examination of the upper few millimeters of the sea when a light breeze is blowing shows surprisingly high velocities at the surface and highly developed vertical shear. Thus soluble dye put into the water becomes separated into a subsurface cloud and a superficial film. The film soon vanishes and the subsurface cloud cannot be relied on as a means of observing motion in the very surface. The best targets tried have been sheets of paper that float nearly horizontally just under the surface. These, when placed in front of an on-coming slick, were observed to be drawn into the slick, and, after some minutes, to be ejected to the rear, indicating that the propagation of slicks does not depend directly on surface flow. Nevertheless, up to the present, the conclusion that slick propagation is a wave phenomenon rests chiefly on the evidence of the model experiment.

The Effect of Wind. Only brief mention will be made of observations showing that calm streaks are oriented independently of wind direction at low wind speeds, because sufficient data are lacking to prove this independence categorically. The intuitive notion that slicks trail downwind like smoke from a chimney must be discarded as a *non sequitur* if the initial distribution of film material is uniform. Only some cross circulation of the wind or water, such as that found by Langmuir (1938) and by Woodcock and Wyman (1947), would produce this orientation, and the cases reported by them appear to involve windspeeds in excess of 4 m/sec. At lower wind speeds, downwind orientation is the least frequently observed of any, most tending to be within 30° of perpendicular to the wind. In shallow water, orienta-

tion of slicks is governed by refraction which tends toward parallelism with the contours of the bottom and of the thermocline, as stated previously. In deeper water, Forbes (1945) has shown that two trains of slicks can coexist with two different orientations, both of which obviously cannot be related to the local surface wind in the same way. Flying across the Gulf of California, the author observed slicks to be oriented about normal to the wind direction. It appears, therefore, that although slicks at low wind speeds are controlled directly by internal waves, these waves may have some preferred orientation nearly normal to the wind. In fact Zeilon (1934), by simulating the condition of a surface current excited by a steady local wind, produced experimental internal waves with crests at right angles to the wind.

DISCUSSION

Nonperiodic Slicks. Calm streaks on the sea surface are caused by a number of agencies other than internal waves. Anything that compresses the film either by mechanical means or by convergent flow will produce this result. Thus a boat sailing through the film splits it into two bands of compressed film that lie on either side of the wake, producing two ribbons of calm in which bubbles are stabilized by the compacted film (Brown, et al., 1949) and which persist much longer than the turbulence of the wake. The attendant drop in surface tension has been measured (Adam, 1937; Shuleikin, 1935, 1941).

Wind stress on the surface produces a zone of calm on the windward side of a barrier (Aitken, 1884; Adam, 1937; Hardman, 1941). The discharge of a river into the sea or into an estuary or pool also produces film accumulation through convergence and hence a calm zone (Thompson, 1862; Aitken, 1884; Adam, 1937; Schmidt, 1936).

A commonly observed slick which is not associated with internal waves forms along the axis or along both sides of tidal channels such as the outer parts of San Diego Harbor or Mission Bay. Similar slicks have been mentioned by Aitken (1884) and by Schmidt (1936) who attribute them to the wind, but this explanation is inadequate in several respects, the most important of which is that they do not usually touch the shore. Preliminary investigation by the author supports the explanation that these channel slicks result from transverse horizontal convergence associated with helicoidal flow along the channel. Such flow is known to occur in rivers below bends and in narrow straight channels with sluggish flow (Hellström, 1948; Gibson, A. H., 1909). It is independent of the wind, being caused by friction along boundaries where these are curved or of asymmetric cross section (Prandtl, 1949; Rouse, 1938: 266–268; Jeffreys, 1929).

In the open ocean, helicoidal flow occurs in the equatorial region (see Sverdrup, et al, 1946; 632–636, 708–712) and in coastal waters (Stockmann, 1946). Since overturn of water is associated with high biological productivity, it is to be expected that in these regions the surface is heavily contaminated with organic film and consequently that a slick should be found along the line of horizontal convergence over that margin of currents which is characterized by subsidence. Where a film is considerably compressed, it acts to stabilize bubbles (Brown, et al, 1949). Under this condition, a region of convergence is revealed more conspicuously by a line of foam than by a slick. Such a foam line is a persistent feature off the U. S. Pacific Coast. It has been photographed and described in detail by Isaacs (1948). A similar line of convergence with attendant slicks has been observed and photographed along the left, or "cold wall," of the Gulf Stream (Kielhorn, 1950). Along the (descending) southern margin of the South Pacific Equatorial Current, a line "3 to 4 feet wide, in the form of a long streak of bubbles and foam reaching as far as the eye could see in an east–west direction" was reported by Heard (1950). A similar narrow streak of foam over 100 miles long was photographed and described in detail by Beebe (1926a, b).

Slicks as an Oceanographic Tool. In considering the uses to which slicks and their relation to internal waves might be put, three stand out. First, slicks may be used to locate regions of horizontal convergence at the sea surface. Second, internal wave slicks represent a map of the distribution of the internal waves and so lend themselves to study of the conditions under which such waves are formed. Third, the fact that at wind speeds greater than 3.4 m/sec the film is dominated by the wind rather than by the motion of the underlying water may shed new light on quantitative aspects of the stress of wind on water.

Inhibition vs. Damping of Ripples. In closing, it is worth pointing out that the calming effect of film on water has been attributed herein solely to variation in the rate at which ripples, once generated, are damped by viscosity of the water. The possible effect of the film on the tangential stress of wind on water has been ignored on the supposition that this is relatively unimportant. It must not be overlooked, however, that careful observations have been reported (Aitken, 1884; Gibson, G. E., 1944) which indicate that the wind-induced surface current is increased by the presence of oil on water. Aitken has suggested that, by distributing the effect of stress from small eddies over areas which are large compared to the length of initially formed ripples, an elastic film discourages the irregular horizontal motion of the water surface which initiates ripple formation, favoring instead a

uniform surface drift. These matters deserve further study. Should it turn out that such variation in the action of wind on water may indeed be induced by surface film, the effects on rippling due to damping would in no way be diminished; on the contrary they would be supplemented.

CONCLUSIONS

1. The surface of coastal waters and of lakes is often coated with film of finely particulate or colloidal material, rich in organic matter.

2. Such films, when in a compact state, lower the surface tension in proportion to the degree of compaction. They therefore make the water surface elastic and increase the rate of dissipation of wave energy for wavelengths from a fraction of a millimeter to several meters. This increase more than doubles the minimum wind velocity required for the growth of waves.

3. Long internal waves in a shallow thermocline produce transient changes of state in a surface film sufficient to form bands of variable surface tension over their troughs. These bands are propagated as a wave with the same velocity as the internal wave.

4. Provided the internal wave be of sufficient amplitude in relation to its depth, light winds (less than Beaufort 3) render the bands visible as long narrow calm streaks in a rippled sea.

5. At wind forces less than 3, internal waves of short period in a shallow thermocline are usually oriented with their long axes nearly perpendicular to the wind except in shallow water where they are refracted by the thermocline or bottom to an orientation nearly parallel to the contours of one or the other of these surfaces.

REFERENCES

Adam, N. K.

1937. A rapid method for determining the lowering of tension of exposed water surfaces, with some observations on the surface tension of the sea and of inland waters. Proc. roy. Soc. London, (B) *122:* 134–139.

1941. The physics and chemistry of surfaces. Oxford University Press, London. 3rd ed. 436 pp.

Aitken, John

1884. On the effect of oil on a stormy sea. Proc. roy. Soc. Edinb., *12:* 56–75.

Beebe, William

1926a. The Arcturus Adventure. Chap. II. G. P. Putnam's Sons, New York. 439 pp.

1926b. The Arcturus oceanographic expedition. Zoologica, N. Y., *8:* 1–45.

Brown, A. G., W. C. Thuman and J. W. McBain

1949. On the stability of single bubbles released under monolayers on water. The physical chemistry and stability of bubbles with special reference to aqueous solution. Stanford Res. Inst. Project 120, Tech. Rep. 3 (T I P abstract U7058).

Devaux, Henri
1914. Oil films on water and on mercury. Rep. Smithson. Instn. (1913): 261–273.
Dietz, R. S. and E. C. LaFond
1950. Natural slicks on the ocean. J. Mar. Res., *9:* 69–76.
Ewing, G. C.
1950. Relation between band slicks at the surface and internal waves in the sea. Science, N. Y., *111:* 91–94.
Forbes, Alexander
1945. Photogrammetry applied to aerology. Photogram. Engng. (1945): 181–192.
Gibson, A. H.
1909. On the depression of the filament of maximum velocity in a stream flowing through an open channel. Proc. roy. Soc. London, (A) *82:* 149–159.
Gibson, G. E.
1944. On an investigation of the calming of waves by means of oil films, carried out at the Woods Hole Oceanographic Institution. Report to the Bureau of Ships (Research and Standards Section).
Hardman, Yvette
1941. The surface tension of Wisconsin lake waters. Trans. Wis. Acad. Sci. Arts Lett., *33:* 395–404.
Heard, P. W.
1950. Current rip, South Pacific. Bull. U. S. Hydrogr. Off., No. 3158.
Hellström, Bo
1948. Macroturbulence in natural stream flow. Trans. Amer. geophys. Un., *29:* 272–274.
Hulburt, E. O.
1934. The polarization of light at sea. J. opt. Soc. Amer., *24:* 35–42.
Isaacs, J. D.
1948. Discussion of "Refraction of surface waves by currents" by J. W. Johnson. Trans. Amer. geophys. Un., *29:* 739–742.
Jeffreys, H.
1925. On the formation of water waves by wind. Proc. roy. Soc. London, (A) *107:* 189–206.
1926. On the formation of water waves by wind. Proc. roy. Soc. London, (A) *110:* 242–247.
1929. Transverse circulation in streams. Proc. Camb. phil. Soc., *25:* 20–25.
Kielhorn, W. V.
1950. A report on aircraft participation in Operation Cabot. U. S. Hydrogr. Off., June 1950 (Unpublished).
Lamb, Horace
1895. Hydrodynamics. Cambridge University Press. 1st ed. 604 pp.
1932. Hydrodynamics. Cambridge University Press. 6th ed. 738 pp.
Langmuir, Irving
1917. The constitution and fundamental properties of solids and liquids. Part 2, Liquids. J. Amer. chem. Soc., *39:* 1848–1906.
1938. Surface motion of water induced by wind. Science, N. Y., *87:* 119–123.

Munk, W. H. and M. A. Traylor
1947. Refraction of ocean waves: a process linking underwater topography to beach erosion. J. Geol., *55:* 1–26.

Pockels, Agnes
1891. Surface tension. Nature, Lond., *43:* 437–439.

Prandtl, Ludwig
1949. Führer durch die Strömungslehre. Friedr. Vieweg & Sohn, Braunschweig. 407 pp.

Reynolds, Osborne
1880. On the effect of oil in destroying waves on the surface of water. Rep. Brit. Ass. (1880): 489–490.

Rouse, Hunter
1938. Fluid mechanics for hydraulic engineers. McGraw-Hill, New York. 422 pp.

Schmidt, Wilhelm
1936. Cause of 'oil patches' on water surfaces. Nature, Lond., *137:* 777.

Shuleikin, V. V.
1935. Active films on the surface of the sea. C. R. Acad. Sci. U. R. S. S., *1* (7/8): 494–501 (Russ. and Eng.).
1941. Fizika Moria. Izdat Akad. Nauk SSSR, Moscow. 833 pp.

Spilhaus, A. F.
1938. A bathythermograph. J. Mar. Res., *1:* 95–100.

Stockmann, W. B.
1946. Characteristic features of the coastal circulation in the sea and their connexion with the transverse non-uniformity of the wind. C. R. (Doklady) Acad. Sci. U. R. S. S., N. S. *54:* 227–230.

Sverdrup, H. U., M. W. Johnson and R. H. Fleming
1946. The Oceans. Prentice-Hall, Inc., N. Y. 1087 pp.

Thompson, James
1862. On the calm lines often seen on a rippled sea. Philos. Mag. (4) 1862: 247–248.

Ufford, C. W.
1947a. Internal waves measured at three stations. Trans. Amer. geophys. Un., *28:* 87–95.
1947b. The theory of internal waves. Trans. Amer. geophys. Un., *28:* 96–101.

Waksman, S. A.
1936. Humus. Williams and Wilkins Co., Baltimore. 494 pp.

Woodcock, A. H. and Jeffries Wyman
1947. Convective motion in air over the sea. Ann. N. Y. Acad. Sci., *48* (8): 749–776.

Zeilon, Nils
1934. Experiments on boundary tides. Göteborg. VetenskSamh. Handl., Folj 5, Ser. B, Bd. 3, No. 10: 8 pp.

ZoBell, C. E.
1946. Marine microbiology. Chronica Botanica Co. Waltham. 240 pp.

POPULATION STUDIES, LOCAL GROWTH RATES AND REPRODUCTION OF THE PISMO CLAM
(*Tivela stultorum*)

By

WESLEY R. COE

Scripps Institution of Oceanography[1]

AND

JOHN E. FITCH

California Division of Fish and Game

ABSTRACT

Large samples collected, measured, and returned to the beach at monthly intervals at La Jolla, California, for five successive years showed an average initial set of 3 young clams per sq m in an area of 2000 sq m. The annual mortality has been from 67 to 75% for each year-class. Of an annual set of 6000, only 2000, 700, 170 and 50, respectively, have remained at the end of the first to fourth years. The length increases about 21 mm per year for the first two years of life and somewhat less thereafter. Less than one per cent survived long enough to reach the legal length of 127 mm.

In the cooler waters of three more northern localities investigated, growth is more rapid, average length of life is longer, and large crops of legal size are produced annually. Population studies by the California Bureau of Marine Fisheries at Pismo Beach for 19 years showed that an average of 50% of those not more than four years old belonged to the first year-class and 23, 13 and 14%, respectively, to the second, third and fourth year-classes. Wide fluctuations occurred. In some years only 0 to 10% of the population belonged to the first year-class, while in other years this year-class comprised 60 to 80%.

The most productive areas on both the California and Mexican coasts are those with extensive upwelling of cool oceanic water, bringing inorganic nutrients essential for the growth of phytoplankton. The principal spawning season is June to December.

The natural populations of this species, which is one of the largest and most palatable of the bivalves on the California coast, have been studied by collecting samples at monthly intervals for five successive years, 1945–1950, on the beach at the Scripps Institution of Oceanography at La Jolla, California. Many marked individuals were also replanted on the beach and remeasured monthly. In addition to this local population, less frequent studies have been made at other localities along the coast for a number of years with the object of determining the population changes from year to year, the sizes and ages of the constituent year-classes, the rates of growth at each locality, the season

[1] Contribution from the Scripps Institution of Oceanography, New Series No. 495.

of spawning and the date of the first appearance of the young clams on the beach.

The Pismo clam inhabits the open coast of the southern half of California and most of the Pacific coast of Lower California. Because of its economic importance, this species has been investigated extensively under the auspices of the California Division of Fish and Game. Weymouth (1923) published a detailed report of its habits, growth and economic aspects. This report was supplemented by Herrington (1930) and population statistics have been published by Clark (1932), Roedel (1939), Aplin (1947), and others. The rates of growth at La Jolla and the nature of the food and its digestion, as well as the sexuality, were described by Coe (1947, 1948), while Fitch (1950) has published a popular account of the ecology, growth and utilization of the clam and the management of the fishery.

In order to determine the extent to which local conditions influence the populations, productivity, rates of growth and the spawning season, collections have been made during each month of the year, with a few exceptions, at four widely separated localities along the coast. The most southern of these are La Jolla and La Jolla Shores, the most northern Pismo Beach, the two being separated by about 215 miles of seacoast. Sunset Beach is about 65 miles northwest of La Jolla, Point Hueneme 65 miles northwest of Sunset Beach, and Pismo Beach about 85 miles further northwest. The season of development of the sexual products and the spawning periods at each of these localities, as well as at Morro Bay and at several beaches on the coast of Lower California, were also investigated. The writers are indebted to Professor and Mrs. Carl L. Hubbs for material and temperature records from some of these more southern localities and to the Bureau of Marine Fisheries for permitting the inclusion of data on the yearly variations in the populations at Pismo Beach obtained by the California Division of Fish and Game.

The constituents of the population and the average lengths of the clams in each of the first four year-classes at each of these localities in samples collected at monthly intervals are shown in Tables I to XIII. The figures given indicate the averages for five years at La Jolla, two to three years at La Jolla Shores, Sunset Beach and Hueneme, and 19 years at Pismo Beach. The mean lengths represent the weighted averages for all of the collections in the corresponding months of successive years. The number of individuals on which the data are based and the average temperature are included.

As an introduction to the present report it may be stated that these clams are generally of separate sexes, with less than one per cent ambisexuality. Weymouth (1923) erroneously reported them as

being hermaphroditic. The principal spawning season extends from June to December, although some individuals may not complete spawning until January and a few may spawn at intervals during the remainder of the year. At La Jolla many of the young clams spawn at the age of about one year, when they are 17 to 31 mm in length, but most of those with retarded growth first become sexually mature in their second summer. At the more northern of the localities investigated, spawning is usually delayed until the clam's second summer or autumn. The older individuals have a prolonged spawning season, discharging their sexual products at intervals during two to six months or more. The ova are very small, measuring only 0.074 to 0.081 mm in diameter, exclusive of the gelatinous membrane, but they are produced in great numbers. A large female may liberate from 10 to 20 million eggs each year for five or more years (Coe, 1947).

After completion of a free-swimming larval period, the minute young clams settle on the beach and remain there unless disturbed by the surf or by enemies. The period of the most successful settling and survival of the young may occur early in the season or one to six months later. Consequently it is usual that in any year-class some individuals are several months older than others.

The constituent year-classes in the population have varied considerably from year to year due to differences in the initial set of young clams and the subsequent mortality. At La Jolla there has been an annual loss of 67 to 75% for each year-class, and less than one per cent of the young clams reached the age of four years. At Pismo Beach, where the water is cooler in summer and conditions for survival much better, the losses have been estimated as 55, 45, 29, 34, 52, 68 and 72%, respectively, for the first to seventh years. The sharp increase in the fifth to seventh years is attributable to the taking of clams of legal size for food. An average of only one clam in each 200 of the original set remains.

The causes, other than human agencies, of this high rate of mortality have not been fully determined. Many of the clams are killed by gulls and others by various species of sharks, rays and bony fishes. Others are drilled by boring snails and some are devoured by cancer crabs, but the highest mortality usually occurs in summer when dinoflagellates are most abundant. At such times vast numbers of clams, particularly those of the first and second year-classes at La Jolla, die from unexplained causes. Dying clams and empty shells may then be left in rows along the shore. Possibly unfavorably high temperature or "disease" may be among the contributing factors. Trematode parasites are common, especially in the older clams, but they are not considered to be seriously detrimental.

During some years the set of young clams on a particular beach has been an almost complete failure and one or more year-classes have been missing from the subsequent population. But whether the mortality has occurred during the larval period or after the settlement of the delicate young clams on the beach at times of heavy surf has not been determined.

Growth is slower than in many bivalves, the average increase at La Jolla being between 21 and 22 mm a year during the first two years of life and somewhat less thereafter (Fig. 1). The legal length of 5 inches

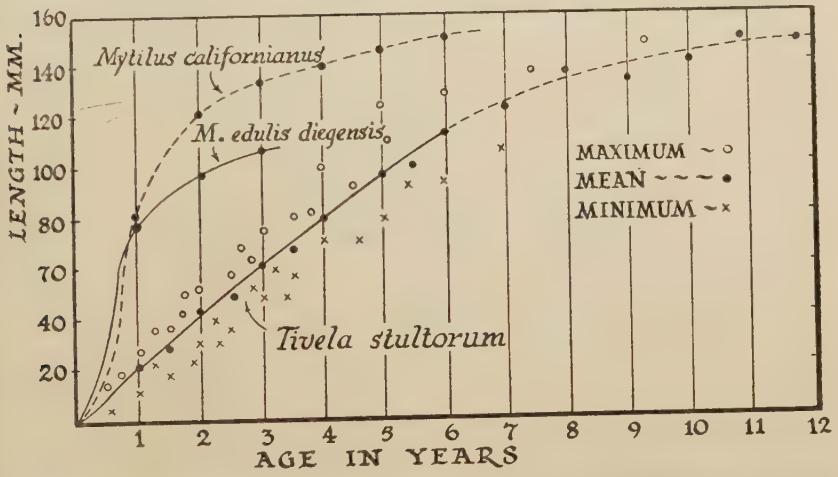

Figure 1. Growth curve of the Pismo clam at La Jolla. Corresponding curves of the growth of the sea-mussel and the bay-mussel from the pier adjacent to the clam beds are indicated for comparison.

is reached in about seven years, while the largest individuals known from La Jolla were 148 to 151 mm long, with an estimated age of 10 years or more. At other localities, lengths of 170 to 175 mm have been found and the age has been estimated as 18 to 25 years. The most rapid increase in length usually occurs during the clam's second year (Table XIII), but the volume and weight increase more rapidly thereafter (Coe, 1947).

Like most other bivalve mollusks, these clams are typical ciliary and mucous feeders, taking into the stomach a great variety of small particles. These include not only living and dead organic materials but also a considerable proportion of sand and small fragments of mollusk shells. The organic material consists mainly of diatoms, dinoflagellates and other unicellular algae, as well as other phytoplankton, both living and dead, protozoans, microflagellates and

bacteria. Detritus derived from the decomposed tissues of all species of marine animals and plants is evidently an important part of the clam's nutrition. However, the experimental studies by Coe (1947, 1948) have shown that only the smallest of these particles and cells without cellulose walls can actually be digested.

INVESTIGATIONS AT LA JOLLA

Collections containing usually about 200 individuals were made near the end of each month, with a few exceptions, during each of the five years. After being measured, the clams were returned to the same part of the beach from which they had been taken. In so far as possible the same individuals were collected in each succeeding month, although most of those that represented the first year-class in 1945 had disappeared before the end of the experimental period in 1950. The number of individuals and the average length and range of those in each year-class for the corresponding months of each year are shown in Tables I and II. It will be noted that the most rapid growth occurs from May to September. During that period the phytoplankton is most abundant and the temperature is highest (Fig. 2). During the winter the growth rate is inhibited by the lower temperature, rougher seas, shifting sand and less abundant nutrition.

The area included in the population studies at La Jolla covered about 2000 square meters of the beach at the Scripps Institution, legally protected from human interference. It is estimated that an average of three young clams arrived on each square meter each year, but the annual decrease in the population has been from 67 to 75% for each year-class. Most of this decrease has been due to destruction by enemies or to death from natural casuses, but a few of the clams were taken by poachers and a relatively small number were carried by the surf into deeper water. Of the average annual set of approximately 6000, only about 2000, 700, 170 and 50 respectively remained at the end of the first to fourth years. The proportions actually collected were 1008, 347, 83 and 25. The constituents of the population found at the end of each month in 1946–47 and the changes which occurred during the year are shown by the diagrams in Fig. 3.

Rates of Growth. In computing the average of the collections at the end of September of these five years, it is found that the 1008 individuals estimated to have an average age of one year had a mean length of 21.5 mm. The lengths varied from 11 to 31 mm (Table I), indicative not only of variations in growth rate but also of differences in actual age because of the prolonged spawning season and the different times of settlement on the beach.

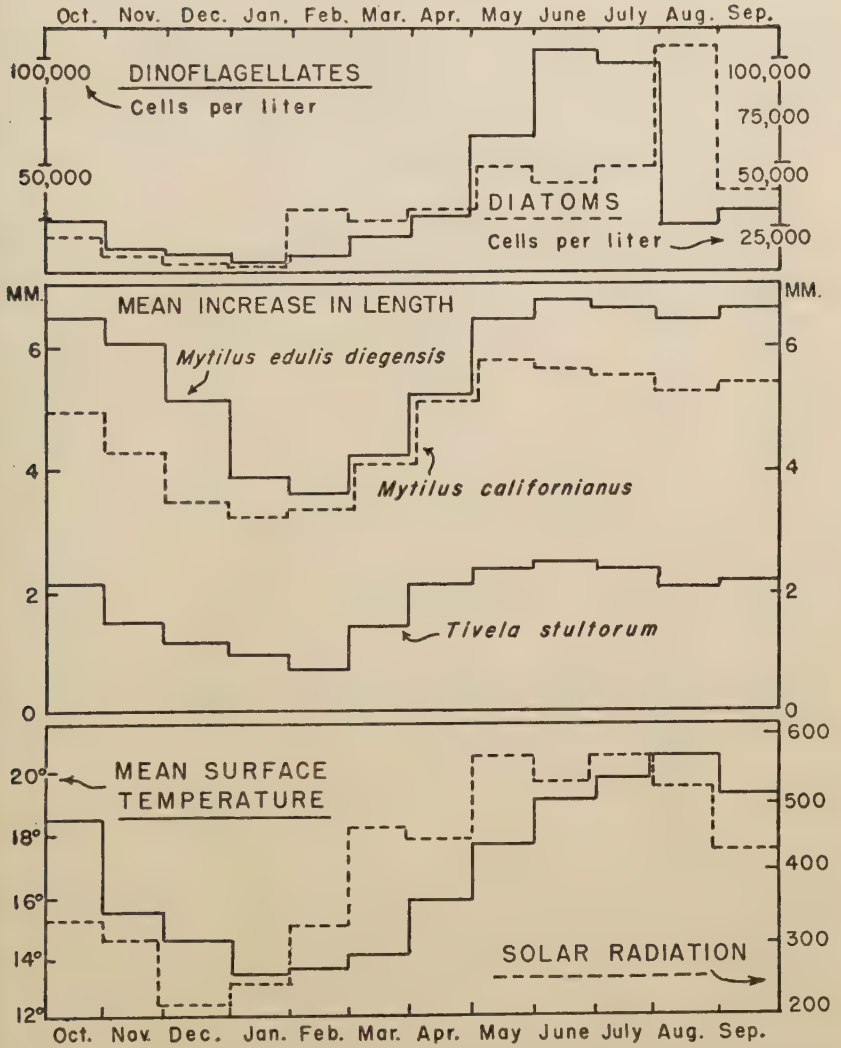

Figure 2. Correlation between temperature, solar radiation, abundance of dinoflagellates and diatoms and mean monthly increase in length at La Jolla during the two years 1945–47. The growth rates are more nearly parallel with the abundance of dinoflagellates than with the other environmental conditions. The incident solar radiation is shown in terms of g. cal./cm²/day. Corresponding curves for the two species of mussels growing on the piles adjacent to the clam beds are indicated for comparison.

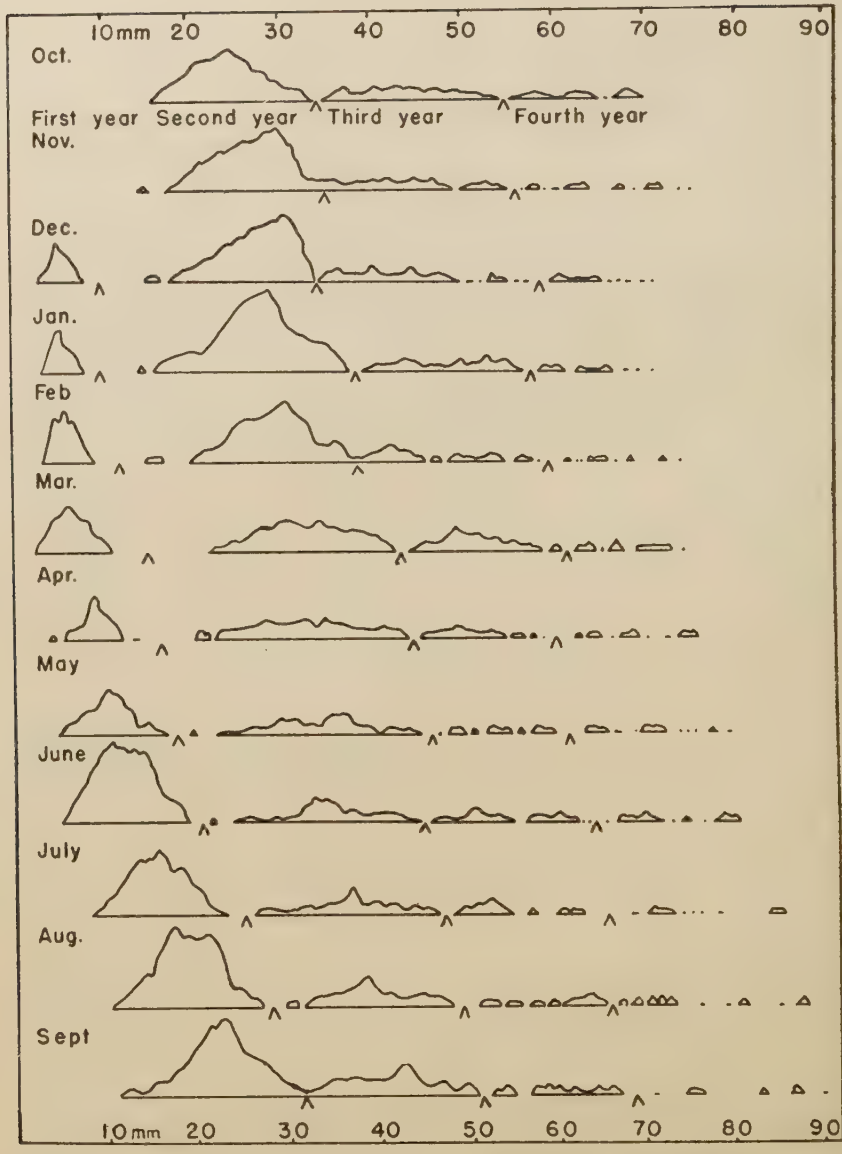

Figure 3. The length-frequency of the first four year-classes in the population at La Jolla during the year 1946–47. as determined from samples collected at the end of each month, October to September. The high mortality is indicated by the rapidly decreasing numbers in each year-class.

At an estimated average age of two years the mean length of 347 individuals had increased to 42.8 mm, indicating an increase of 21.3 mm during the second year. This is only slightly less than during the first year. The relative number of individuals two years old in the population, however, had decreased to but little more than a third of those found in the first year-class. The maximum length at the end of the second year was 52 mm and the minimum 29 mm (Table I).

TABLE I.—Rates of Growth at La Jolla During First and Second Years

Date	*Average water temperature*	*Average age, months*	*Number in samples*	*Length, mm*		*Indicated increase in month*
				Mean	*Range*	
October	18.26	1	—	—	—	—
November	15.58	2	—	—	—	—
December	14.15	3	368	4.8	3–7	—
January	13.08	4	145	5.6	4–12	0.8
February	13.11	5	107	6.5	4–12	0.9
March	13.84	6	457	7.6	4–13	1.1
April	15.28	7	144	9.4	4–18	1.8
May	17.36	8	491	11.7	5–22	2.3
June	18.88	9	813	14.3	6–22	2.6
July	19.57	10	1016	16.7	7–26	2.4
August	20.48	11	1183	19.0	11–30	2.3
September	19.64	12	1008	21.5	11–31	2.5
October	18.26	13	217	23.4	15–33	1.9
November	15.58	14	602	25.0	15–35	1.6
December	14.15	15	548	26.4	15–38	1.4
January	13.08	16	646	27.4	17–39	1.0
February	13.11	17	514	28.5	15–39	1.1
March	13.84	18	521	30.1	17–41	1.6
April	15.28	19	434	32.4	22–43	2.3
May	17.36	20	362	33.7	20–45	1.3
June	18.88	21	281	36.0	22–46	2.3
July	19.57	22	273	38.2	24–49	2.2
August	20.48	23	184	40.4	28–50	2.2
September	19.64	24	347	42.8	29–52	2.4

In the collections made at the end of September, 1945–1949, only 83 individuals were found with an estimated age of three years. Their average length was 62.0 mm, indicating a mean increase of 19.2 mm during the third year. The maximum was 68 mm and the minimum 52 (Tables II and III).

At the average age of four years the lengths varied between 67 and 95 mm, with a mean of 78.9 mm, indicating an increase of 16.9 mm during the fourth year (Table III).

Marked Individuals. A reliable measurement of the growth rates from month to month was obtained by marking the shells of more than 800 clams and replanting them on the beach. From those that were recovered subsequently it was found that the average increase in

TABLE II.—Rates of Growth at La Jolla During Third and Fourth Years

Date	*Average water temperature*	*Average age, months*	*Number in samples*	*Length, mm* Mean	Range	*Indicated increase in month*
October	18.26	25	73	44.6	31–53	1.8
November	15.58	26	94	45.9	35–55	1.3
December	14.15	27	106	47.1	35–55	1.2
January	13.08	28	92	47.0	35–56	−0.1
February	12.11	29	104	48.1	38–59	1.1
March	13.84	30	128	50.3	39–62	2.2
April	15.28	31	91	52.1	42–58	1.8
May	17.36	32	76	54.1	44–61	2.0
June	18.88	33	68	56.3	46–63	2.2
July	19.57	34	64	58.4	49–65	2.1
August	20.48	35	61	60.1	50–65	1.7
September	19.64	36	83	62.0	52–68	1.9
October	18.26	37	37	63.1	57–69	1.1
November	15.58	38	29	64.1	57–78	1.0
December	14.15	39	26	64.0	60–70	−0.1
January	13.08	40	23	65.8	59–71	1.8
February	13.11	41	28	66.9	59–73	1.1
March	13.84	42	24	68.4	62–74	1.5
April	15.28	43	25	70.3	62–76	1.9
May	17.36	44	24	72.4	63–79	2.1
June	18.88	45	24	74.4	64–80	2.0
July	19.57	46	19	76.2	66–86	1.8
August	20.48	47	20	76.9	67–89	0.7
September	19.64	48	25	78.9	67–95	2.0

TABLE III.—Relative Proportions of the Population in Each Age Group and Yearly Increment in Length (mm) at La Jolla in First, Second, Third and Fourth Years, as Estimated from Samples Collected at End of September in Each Year

Year	*Av. age, 1 year*		*Av. age, 2 years*			*Av. age, 3 years*			*Av. age, 4 years*		
	No. in sample	*Av. length*	*No. in sample*	*Av. length*	*Inc.*	*No. in sample*	*Av. length*	*Inc.*	*No. in sample*	*Av. length*	*Inc.*
1945	135	20.9	38	42.0	—	21	58.5	—	3	77.3	—
1946	247	21.2	61	42.3	21.4	12	61.8	19.8	3	78.4	19.9
1947	214	21.4	71	41.1	19.9	8	59.1	16.8	4	81.1	19.3
1948	211	20.7	82	43.1	21.7	19	62.0	20.9	6	75.2	16.1
1949	141	23.3	95	45.3	22.2	23	68.6	19.3	9	82.4	12.3
Total	1008	—	347	—	—	83	—	—	25	—	—
Aver.	—	21.5	—	42.8	21.3	—	62.0	19.2	—	78.9	16.9

length in their second and third years was 2.1 mm in October, 1.7 mm in November, 1.2 mm in December, 0.9 mm in January, 0.7 mm in February, 1.2 mm in March, 2.0 mm in April, 2.3 mm in May, 2.4 mm in June, 2.3 mm in July, 2.0 mm in August, and 2.3 mm in September. These figures indicate an increase of only 7.8 mm for the six months preceding the end of March and 13.3 mm during the following half year, the increment for the entire year being 21.1 mm (Fig. 2). This would average 1.3 mm per month in winter and 2.2 mm per month in summer.

INVESTIGATIONS AT LA JOLLA SHORES

On this beach, which is only a mile from the one at the Scripps Institution, there has been only occasional patrol by the wardens of the California Division of Fish and Game and this has not prevented the public from taking as many young clams of illegal size as could be found. Consequently there is a less natural population and the collections, which were made at intervals over several years, show much less uniformity. The temperature and other environmental conditions at the two localities are essentially similar, except that in spite of the relatively large numbers in the first and second year-classes only a few individuals have been permitted to reach their third year and nearly all have been taken from the beach before the end of their fourth year (Tables IV and V). The population has been maintained by the spawning of such young individuals as have escaped the public and by older ones living in deeper water or on other beaches.

TABLE IV.—Rates of Growth at La Jolla Shores During First and Second Years

Date	*Average age, months*	*Number in samples*	*Length, mm*		*Indicated increase in month*
			Mean	*Range*	
October	1	—	—	—	—
November	2	—	—	—	—
December	3	8	7.2	5–9	—
January	4	33	8.5	4–13	1.3
February	5	83	8.1	2–13	−0.4
March	6	13	10.8	6–17	2.7
April	7	38	10.1	7–17	−0.7
May	8	317	9.7	3–22	−0.4
June	9	241	11.7	2–24	2.0
July	10	686	11.1	3–25	−0.6
August	11	330	14.3	6–27	3.2
September	12	234	20.2	13–20	5.9
October	13	467	19.9	9–34	−0.3
November	14	473	21.5	11–36	1.6
December	15	464	24.6	10–38	3.1
January	16	446	25.5	14–40	0.9
February	17	258	28.3	15–42	2.8
March	18	80	31.2	23–39	2.9
April	19	116	31.0	19–45	−0.2
May	20	212	34.0	21–45	3.0
June	21	103	36.9	29–48	2.9
July	22	261	38.6	26–48	1.7
August	23	278	39.7	25–53	1.1
September	24	87	40.8	31–53	1.1

The average lengths at the end of the first, second and third years were 20.2, 40.8 and 63.7 respectively at La Jolla Shores as compared with 21.5, 42.8 and 62.0 mm at La Jolla. These small differences do not exceed the probable errors to be expected in random samples (Tables IV and V).

TABLE V.—Rates of Growth at La Jolla Shores during Third and Fourth Years

Date	*Average age, months*	*Number in samples*	*Length, mm*		*Indicated increase in month*
			Mean	*Range*	
October	25	290	40.4	29–58	−0.3
November	26	103	42.3	32–63	1.9
December	27	72	44.0	34–56	1.7
January	28	95	47.2	38–61	3.2
February	29	49	49.9	44–63	2.7
March	30	19	45.4	41–55	4.5
April	31	34	53.2	46–61	7.8
May	32	47	50.9	44–59	−2.3
June	33	13	58.6	51–66	7.7
July	34	55	54.5	47.68	−4.1
August	35	29	60.0	51–68	5.5
September	36	15	63.7	56–77	3.7
October	37	54	61.2	53–81	−2.5
November	38	8	63.6	59–68	2.4
December	39	2	64.5	63–66	0.9
January	40	5	66.6	59–81	2.1
February	41	5	71.0	67–78	4.4
March	42	—	—	—	—
April	43	—	—	—	—
May	44	—	—	—	—
June	45	5	73.6	68–81	—
July	46	2	79.5	71–88	5.9
August	47	6	72.8	71–75	−6.7
September	48	—	—	—	—

In some months the collections on the two beaches were nearly identical, while in other months there was a wide difference in the proportions of the year-classes. One curious difference deserves special emphasis. A comparison of Tables I and IV shows that some individuals of the first year-class only 3 mm in length continued to be found as late as July at La Jolla Shores, while none of that small size have been discovered at La Jolla later than the preceding December. A length of 3 mm would normally indicate an individual less than two months after setting, giving evidence that spawning may occasionally continue as late as March or April. At that time the gonads of most of the population are in various stages of gametogenesis preparatory to the more usual spawning season, June to December.

INVESTIGATIONS AT SUNSET BEACH

This locality, about 65 miles northwest of La Jolla, has been particularly favorable for the rapid growth of the clam, presumably because of the large sewer which brings to the vicinity an abundance of nutrients from the wastes of a dense human population. The temperature of the water at nearby Balboa Pier averages only slightly lower than that at La Jolla (Tables VI, VII and XIII). The mean length at the estimated average age of one year was found to be 26.9

TABLE VI.—Rates of Growth at Sunset Beach during First and Second Years

Date	*Average water* temperature*	*Average age, months*	*Number in samples*	*Length, mm*		*Indicated increase in month*
				Mean	*Range*	
October	16.72	1	—	—	—	—
November	15.07	2	—	—	—	—
December	13.76	3	—	—	—	—
January	12.13	4	—	—	—	—
February	12.31	5	3	5.3	4–6	—
March	12.96	6	—	—	—	—
April	14.37	7	1	8	8	—
May	17.19	8	208	7.3	4–20	−0.7
June	19.05	9	557	13.4	5–27	6.1
July	18.95	10	127	14.0	6–25	0.6
August	19.24	11	141	21.0	16–32	7.0
September	18.62	12	128	26.9	19–35	5.9
October	16.72	13	284	30.9	21.45	4.0
November	15.07	14	204	21.7	24–41	0.8
December	13.76	15	279	36.8	21–49	5.1
January	12.13	16	162	34.5	21–49	−2.3
February	12.31	17	140	37.6	27–43	3.1
March	12.96	18	—	—	—	—
April	14.37	19	20	42.3	36–51	—
May	17.19	20	202	47.0	40–57	4.7
June	19.05	21	278	53.8	42–75	6.8
July	18.95	22	316	57.6	42–70	3.8
August	19.24	23	54	61.5	47–70	3.9
September	18.62	24	133	65.2	46–77	3.7

* At Balboa Pier, 1948–49

mm, as compared with 21.5 mm at La Jolla. The average length at the estimated age of two years was 65.2 mm, as compared with 42.8 at La Jolla, while those clams believed to be three years old averaged 88.5 mm, with a maximum of 102 mm. During the fourth year the lengths varied from 78 to 122 mm, with an average of 103.8 mm at the end of the year (Table VII).

These data would indicate an average increase of 26.9 mm during the first year, 38.3 mm in the second, 23.3 mm in the third, and 15.3 mm in the fourth year (Table XIII). This last figure is obviously not representative, since it was based on only 6 individuals and is smaller than indicated for the same year-class three months earlier (Tables VI and VII). The disappearance of this year-class is attributed to removal of clams of both legal and illegal sizes from this beach by the public.

To determine whether the rapid growth rate was due to the environmental conditions or to different genetic factors in the population, more than 100 individuals were marked as to size and transplanted from this beach to La Jolla at various times. They grew somewhat more rapidly for two or three months than clams of similar size in the native population near which they were planted. However, after a few months those from Sunset Beach grew no faster than their native

TABLE VII.—Rates of Growth at Sunset Beach during Third and Fourth Years

Date	*Average water* temperature*	*Average age, months*	*Number in samples*	*Length, mm* *Mean*	*Range*	*Indicated increase in month*
October	16.72	25	170	67.0	50–77	1.8
November	15.07	26	68	65.0	53–79	−2.0
December	13.76	27	278	70.1	50–82	4.9
January	12.13	28	244	70.1	54–88	0.0
February	12.31	29	283	70.1	55–88	0.0
March	12.96	30	—	—	—	—
April	14.37	31	154	73.0	59–88	—
May	17.19	32	427	75.0	58–91	2.0
June	19.05	33	294	78.4	64–94	3.4
July	18.95	34	226	82.8	69–97	4.4
August	19.24	35	256	85.2	74–99	2.4
September	18.62	36	243	88.5	69–102	3.3
October	16.72	37	197	89.2	78–101	0.7
November	15.07	38	26	93.7	79–103	4.5
December	13.76	39	347	95.6	82–116	1.9
January	12.13	40	137	96.9	85–115	1.3
February	12.31	41	145	96.5	84–115	−0.4
March	12.96	42	—	—	—	—
April	14.37	43	135	100.7	89–122	—
May	17.19	44	120	99.5	87–118	−1.2
June	19.05	45	94	104.1	92–121	4.6
July	18.95	46	94	103.1	92–117	−1.0
August	19.24	47	—	—	—	—
September	18.62	48	6	103.8	97–110	—

* At Balboa Pier, 1948–49

associates. It is therefore concluded that the increased growth rate of the population at Sunset Beach results from the favorable environmental conditions and not from different hereditary characteristics.

Although the spawning season is approximately the same as that at La Jolla, no representatives of the new set have been found until February and only four individuals until May. The size in the latter month (4 to 20 mm) obviously indicates a group present earlier but previously overlooked. All were fully ripe or partly spawned out in August.

INVESTIGATIONS AT POINT HUENEME

Point Hueneme is only about 130 miles northwest of La Jolla, but the temperature of the water is generally considerably lower. The differences vary with the season, and in most years the temperatures are only 1 to 2° C lower than those at La Jolla during the winter but are commonly 3 to 4° lower during the summer and autumn months when most of the clams are spawning and when they have the most rapid rate of growth (Tables VIII and IX). These temperatures were taken on the open coast, however, and are several degrees lower than those at the clam beds on sunny afternoons.

Nevertheless, it would appear that the clams increase in size more rapidly than at any of the other localities with the exception of Sunset Beach (Tables VIII and IX). It seems probable that the low summer temperatures indicate the upwelling of oceanic water, bringing to that area inorganic nutrients favorable for an initial growth of phytoplankton and indirectly for the microorganisms and detritus on which the clam's nutrition depends. The average spawning season is about two months later than at La Jolla.

TABLE VIII.—Rates of Growth at Point Hueneme during First and Second Years

Date	*Average water* temperature*	*Average age, months*	*Number in samples*	*Length, mm*		*Indicated increase in month*
				Mean	*Range*	
December	12.95	1	—	—	—	—
January	11.10	2	—	—	—	—
February	11.43	3	—	—	—	—
March	12.25	4	—	—	—	—
April	13.05	5	—	—	—	—
May	14.80	6	—	—	—	—
June	15.03	7	46	10.2	4–15	—
July	16.30	8	120	9.0	4–21	−1.2
August	16.04	9	225	13.0	5–28	4.0
September	16.61	10	—	—	—	—
October	15.34	11	1	22.0	22	—
November	14.82	12	35	23.4	11–32	1.4
December	12.95	13	—	—	—	—
January	11.10	14	208	35.0	20–44	—
February	11.43	15	200	38.6	28–49	3.6
March	12.25	16	—	—	—	—
April	13.05	17	152	41.3	33–52	—
May	14.80	18	153	46.3	28–57	5.0
June	15.03	19	150	50.4	28–58	4.1
July	16.30	20	172	54.9	39–66	4.5
August	16.04	21	152	56.5	45–66	1.6
September	16.61	22	—	—	—	—
October	15.34	23	198	61.4	43–72	—
November	14.82	24	156	60.9	48–72	−0.5

* 1948–49

At the estimated average of one year the mean length in a small collection was only 23.4 mm, but a large collection two months later showed a mean of 35.0 mm. At the end of the second year the mean length was 60.9 mm as compared with 42.8 mm at La Jolla. The indicated mean increase of 37.5 mm in one year makes it seem probable that the small collection at the end of the first year represented a sample of smaller sizes than the normal average at that locality (Table XIII).

At the end of the third year the mean length was 86.7 mm, indicating an increase of 25.8 mm during the year. In the fourth year an apparent gain of 17.5 mm brought the mean length to 104.2 mm (Table IX).

TABLE IX.—Rates of Growth at Point Hueneme during Third and Fourth Years

Date	*Average water* temperature*	*Average age, months*	*Number in samples*	*Length, mm* Mean	Range	*Indicated increase in month*
December	12.95	25	—	—	—	—
January	11.10	26	270	64.4	52–78	—
February	11.43	27	49	67.3	56–77	2.9
March	12.25	28	203	67.3	55–79	0.0
April	13.05	29	35	67.4	54–79	0.1
May	14.80	30	215	71.4	58–85	4.0
June	15.03	31	154	74.8	61–89	3.4
July	16.30	32	116	78.0	66–91	3.2
August	16.04	33	114	80.4	67–95	2.4
September	16.61	34	—	—	—	—
October	15.34	35	5	85.0	77–94	—
November	14.82	36	53	86.7	73–100	1.7
December	12.95	37	—	—	—	—
January	11.10	38	33	89.6	76–111	—
February	11.43	39	11	84.9	79–97	−4.7
March	12.25	40	—	—	—	—
April	13.05	41	15	86.7	80–103	—
May	14.80	42	42	87.3	78–105	0.6
June	15.03	43	23	90.5	84–104	3.2
July	16.30	44	52	94.4	83–114	3.9
August	16.04	45	16	99.2	93–110	4.8
September	16.61	46	—	—	—	—
October	15.34	47	—	—	—	—
November	14.82	48	5	104.2	101–111	—

* 1948–49

Spawning by most individuals had been nearly completed in January. Gametogenesis in February and March was usual, although a few were apparently ripe or partially spawned out. Most individuals were apparently ripe in May. Spawning by both sexes took place in the aquarium on June 10, and the eggs produced normal larvae. All were fully ripe or partly spawned out in August.

INVESTIGATIONS AT PISMO BEACH

This beach has long been noted as one of the most productive localities on the California coast. The investigations of Weymouth (1923), Herrington (1930), Clark (1932) and Roedel (1939) were made in this area, and population studies have been continued in subsequent years by the California Bureau of Marine Fisheries.

Weymouth concluded from an examination of the growth rings that the average length of the young clams at Pismo Beach and Oceano during the first winter, when he supposed they were 4 to 6 months of age, was 22 mm and during the second winter 45 mm, but he was doubtless in error as to the ages. Our data show a mean length of 19.0 mm at the estimated age of one year and 46.7 mm at the age of two years (Tables X and XIII). This would indicate an increase of 27.7 mm

during the second year. The average increment in the third year was 21.1 mm and in the fourth year 19.3 mm (Tables XI and XIII).

TABLE X.—Rates of Growth at Pismo Beach during First and Second Years, Including Data from Weymouth (1923) and the California State Fisheries Laboratory

Date	*Average water* temperature*	*Average age, months*	*Number in samples*	*Length, mm*		*Indicated increase in month*
				Mean	*Range*	
December	12.86	1	—	—	—	—
January	12.10	2	—	—	—	—
February	11.91	3	—	—	—	—
March	11.46	4	—	—	—	—
April	10.69	5	—	—	—	—
May	11.31	6	—	—	—	—
June	11.90	7	—	—	—	—
July	12.35	8	31	7.4	4–13	—
August	12.93	9	—	—	—	—
September	13.58	10	169	13.4	6–23	—
October	13.54	11	—	—	—	—
November	12.99	12	4232	19.0	8–36	—
December	12.86	13	44	21.2	16–25	2.2
January	12.10	14	143	27.2	12–32	6.0
February	11.91	15	231	24.5	14–36	−2.7
March	11.46	16	381	29.7	24–35	5.2
April	10.69	17	187	30.0	23–37	0.3
May	11.31	18	285	32.7	25–40	2.7
June	11.90	19	344	34.9	21–43	2.2
July	12.35	20	593	38.1	12–49	3.2
August	12.93	21	152	45.7	39–53	7.6
September	13.58	22	224	43.9	23–55	−1.8
October	13.54	23	141	49.6	42–56	5.7
November	12.99	24	2483	46.7	32–65	−2.9

* At Point Arguello

Although no data are available as to the temperature of the water directly adjacent to Pismo Beach, the mean annual temperature of the water a few miles offshore in that area averages about 13° C as compared with 16.9° at La Jolla. In October, when it is probable that the greatest number of larvae are in the water, the average temperature is only 13 to 15° and falls to 12° or lower during the winter. In some years it does not reach as high as 13° until July. At Point Arguello, only about 30 miles south of Pismo Beach, the temperature at the shore is even lower, with a yearly average of only 12.3°. The monthly average reaches as high as 13° in September and October only, while at La Jolla during these two months the average temperature of the water is 6 to 7° higher. It should be emphasized that on sunny afternoons the temperature of the water on the beach at Pismo may sometimes rise as high as 24° C and that of the sand at the level occupied by the clams may be above 21° (Weymouth, 1923).

Weymouth concluded that the spawning season at Pismo Beach

TABLE XI.—Rates of Growth at Pismo Beach during Third and Fourth Years, Including Data from Weymouth (1923) and the California State Fisheries Laboratory

Date	*Average water* temperature*	*Average age, months*	*Number in samples*	*Length, mm*		*Indicated increase in month*
				Mean	*Range*	
December	12.86	25	16	54.5	50–60	7.8
January	13.10	26	63	53.7	39–62	−0.8
February	11.91	27	264	52.3	40–66	−1.4
March	11.46	28	16	60.6	52–70	8.3
April	10.69	29	45	58.9	44–69	−1.7
May	11.31	30	106	62.8	47–70	3.9
June	11.90	31	195	62.5	45–80	−0.3
July	12.35	32	81	66.9	48–78	4.4
August	12.93	33	88	74.2	55–80	7.3
September	13.58	34	—	—	—	—
October	13.54	35	35	77.4	67–81	—
November	12.99	36	1369	67.8	64–85	−9.6
December	12.86	37	—	—	—	—
January	12.10	38	233	77.2	59–91	—
February	11.91	39	60	77.1	63–89	−0.1
March	11.46	40	—	—	—	—
April	10.69	41	136	82.0	68–98	—
May	11.31	42	323	84.2	71–96	2.2
June	11.90	43	150	90.0	77–104	5.8
July	12.35	44	175	92.2	77–107	2.2
August	12.93	45	160	91.1	80–104	−1.1
September	13.58	46	—	—	—	—
October	13.54	47	—	—	—	—
November	12.99	48	1141	87.1	—	—

* At Point Arguello

extends from July to September, although he found large eggs in some of the individuals which he examined at intervals from March to November. It has now been found, however, that while the most active spawning takes place in the summer and autumn, apparently normal ovogenesis and spermatogenesis continue in some members of the population throughout the entire year. This is not considered satisfactory proof that spawning actually takes place in midwinter and early spring, although the gonads of a small proportion of the individuals examined indicated such an occurrence. This evidence is corroborated by finding young clams only 4 mm long in July and 6 mm long in September (Table X).

The earliest observed spawning by clams from this beach occurred in the aquarium in June. But no young clams have yet been found on this beach until July of the following year. They had then attained a length of 4 to 13 mm, with a mean of 7.4 mm (Table X). Assuming a rate of increase of 1 mm a month in winter and 1.7 in the spring, it would have required about eight months to reach a length of 13 mm. Consequently, a mean of 7.4 mm in July would indicate a population

averaging five to six months of age. The data for the remainder of the year are in harmony with this assumption. For these reasons it is concluded that the median date when the young have completed the larval period and settled on the beach at Pismo Beach is November, or about two months later than at La Jolla. They would then have an average age of one month in December, but presumably these dates vary considerably in different years.

The estimated sizes and ages of the clams found in equal sections of Pismo Beach by the California Bureau of Marine Fisheries in the census taken in November of each of the years 1927 to 1949, with the exception of 1942 to 1945 and 1948, are indicated in Table XII. The

TABLE XII.—Average Length and Yearly Increment of Clams in the First Four Age Groups Collected at Pismo Beach in November of Each Year by the California Bureau of Marine Fisheries

	Av. age, 1 year		*Av. age, 2 years*			*Av. age, 3 years*			*Av. age, 4 years*		
Year	*No. in sample*	*Av. length*	*No. in sample*	*Av. length*	*Inc.*	*No. in sample*	*Av. length*	*Inc.*	*No. in sample*	*Av. length*	*Inc.*
1927	38	22.9	62	44.7	—	28	66.7	—	21	88.3	—
1928	6	22.7	32	43.1	20.2	40	61.6	16.9	23	86.5	19.8
1929	468	20.1	5	40.8	18.1	23	59.0	15.9	23	83.1	21.5
1930	357	20.1	189	43.3	23.2	5	68.2	27.4	4	84.5	25.5
1931	871	21.7	149	43.0	22.9	56	62.7	19.4	—	—	—
1932	44	21.5	279	44.5	22.8	128	63.8	20.8	103	80.8	18.1
1933	199	15.3	38	46.1	24.6	122	63.8	19.3	98	75.1	11.3
1934	0	—	70	42.6	27.3	23	69.8	23.7	80	87.6	23.8
1935	758	18.0	2	44.0	—	56	63.0	20.4	14	85.3	15.5
1936	142	21.6	270	42.6	24.6	3	63.0	19.0	45	79.2	16.2
1937	743	14.9	101	45.7	24.1	245	62.3	19.7	8	75.1	12.1
1938	9	25.6	231	38.5	23.6	90	62.4	16.7	173	82.3	20.0
1939	23	17.3	4	41.8	16.2	53	57.6	19.1	75	87.0	24.6
1940	24	21.9	34	45.2	27.8	11	70.9	29.1	19	87.1	29.5
1941	13	20.0	4	41.8	19.9	3	68.7	23.5	—	—	—
1942	—	—	—	—	—	—	—	—	—	—	—
1943	—	—	—	—	—	—	—	—	—	—	—
1944	—	—	—	—	—	—	—	—	—	—	—
1945	—	—	—	—	—	—	—	—	—	—	—
1946	384	19.4	164	49.8	—	57	73.3	—	200	92.8	—
1947	31	19.7	297	49.0	29.6	101	75.7	25.9	65	93.5	20.2
1948	—	—	—	—	—	—	—	—	—	—	—
1949	1	13.0	7	43.0	28.9	53	75.0	20.7	19	92.8	16.7
Totals	4111		1938			1097			1141		
Av. length		18.9		44.4			65.2			86.6	
Av. increase		—			25.5			20.8			21.4

total of 4111 clams approximately one year of age had a mean length of 18.9 mm. Those two, three and four years old numbered 1938, 1097 and 1141 respectively, with average lengths of 44.4, 65.2 and 86.6 mm. The clams at La Jolla at the corresponding ages had average lengths of 21.5, 42.8, 62.0 and 78.9 mm. With the exception of the first group, the rates of growth were somewhat greater at Pismo Beach than at La Jolla. At Pismo Beach, moreover, the number of clams which

were four years old was even larger than in the group one year younger, while at La Jolla relatively few individuals survive in the intertidal zone for more than three years.

Since all of the collections made by the Bureau of Marine Fisheries covered equal amounts of space in the same location on the beach in successive years, the numbers in each year-class will indicate the changes in the population from year to year. Inspection of Table XII will show that the numbers in the first year-class varied from 0 in 1934 and 1 in 1949 to 871 in 1931, the total number for the 19 years being 4111, or 50% of the total of 8287 for the four year-classes. The average lengths, omitting the single individual found in 1949, varied from 14.9 mm in 1937 to 22.9 mm in 1927 and 25.6 mm for the small number found in 1938.

The second year-class varied in number from 2 in 1935, 4 in 1939 and 1941, and 5 in 1929 to 279 in 1932 and 297 in 1947. The total number in the second year-class was 1938 or approximately 23% of the entire population of 8287 individuals not exceeding four years of age. The average lengths varied from 38.5 mm in 1938 to 49.8 mm in 1946, while the mean length at the end of the second year was 44.4 mm, indicating an average increase during the second year of 25.5 mm (Table XII).

Similarly, the third year-class varied in number from 3 in 1936 and 1941 and 5 in 1930 to 245 in 1937, the total number being 1097 or approximately 13% of the entire population not exceeding four years of age. The average lengths at the estimated average age of three years varied from 57.6 mm in 1939 to 75.7 mm in 1947, with a mean of 65.2 mm.

Of the fourth year-class, 1141 individuals were obtained. These represent about 14% of the entire collections. The numbers varied from 0 in 1931 and 4 in 1930 to 200 in 1946. The average lengths at the estimated average age of four years ranged from 75.1 mm in 1933 and 1937 to 93.5 mm in 1947, the mean length being 86.6 mm (Table XII).

These extensive collections afford excellent examples of the great variability that may be expected in dealing with populations of invertebrates, not only in the constituent year-classes, as shown in Fig. 4, but also in the rates of growth in successive years. An estimate of the rate of survival through the first four years of life may be obtained from Table XII. It is obvious that any first year-class will be followed by the second year-class in the line below, which gives the data for the following year, and so on. Hence, if the figures in Table XII be read obliquely downward and to the right they will show the fate of any

first year-class in following years in so far as could be determined by the collections taken from equal areas of the beach in successive years.

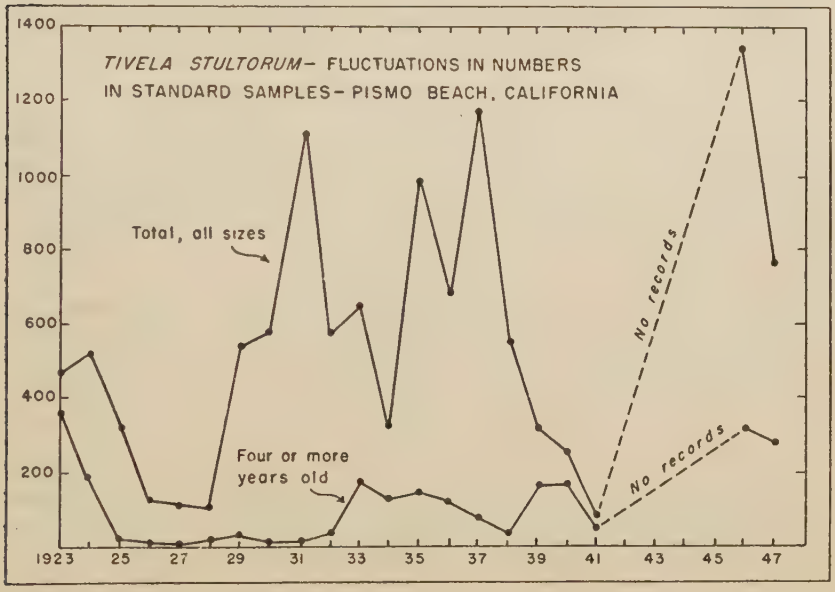

Figure 4. Fluctuations in the populations found each year in three trenches, each 16 cm. wide, in separate locations on Pismo Beach, California, at corresponding dates, 1923–1941 and 1946–47. Between 1930 and 1938 the total population showed a biennial periodicity due to an increased set of young clams in each alternate year. The relatively small number of clams reaching the age of four or more years indicates the high rate of mortality due to natural causes and human agency. (Data from Aplin, 1947 and from California State Fisheries Laboratory.)

TABLE XIII.—Comparative Growth Rates of the First Four Year-classes at Five Localities

	Mean annual temp. of water[1]	*Average length at each age, mm*				*Average annual increment, mm*			
		1 yr.	*2 yr.*	*3 yr.*	*4 yr.*	*1 yr.*	*2 yr.*	*3 yr.*	*4 yr.*
La Jolla	16.94° C	21.5	42.8	62.0	78.9	21.5	21.3	19.2	16.9
La Jolla Shores	16.94	20.2	40.8	63.7	—	20.2	20.6	22.9	—
Sunset Beach	16.58	26.9	65.2	88.5	103.8	26.9	38.3	23.3	15.3
Hueneme	14.71	23.4	60.9	86.7	104.2	23.4	37.5	25.8	17.5
Pismo Beach	12.30	18.9	44.4	65.2	86.6	18.9	25.5	20.8	21.4

[1] At nearest temperature station, usually on a pier.

Table XIII gives a comparison of the growth rates at the five localities investigated, as indicated by the average lengths and the annual increases of the first four year-classes, including all collections. It will be noted that the most rapid growth was found at Sunset Beach, with

the rate at Hueneme nearly as great and at Pismo Beach considerably less. La Jolla and La Jolla Shores, with the highest temperatures, appear to be less favorable for rapid growth and long survival than the localities with cooler water farther north or where there is extensive upwelling of cool oceanic water farther south along the Mexican Coast.

INVESTIGATIONS AT OTHER LOCALITIES

Morro Bay. The cool water at this locality is conducive to large populations of clams of legal size. In January most individuals were near the end of the spawning period or were completely spawned out, although a small percentage was continuing active gametogenesis. In February the spawned out condition predominated and in March all stages of gametogenesis were general, leading to the apparently ripe condition of some individuals in April. The first spawning observed in the aquarium was in June, although the gonads of others showed that spawning had occurred previously.

LOWER CALIFORNIA

On some of the beaches from 100 to 500 miles south of the Mexican border there is extensive upwelling of cool oceanic water and large populations of this species are produced. Collections from the following localities have been examined at intervals.

Punta Cabras (31° 20′ N. Lat.). At this locality, about 100 miles south of the Mexican border, there is extensive upwelling of cool oceanic water, with a thriving population of clams which reach a large size. All of the clams examined in February were completely spawned out and others obtained in April had only early gametogenesis. Most of those examined in May showed early gametogenesis, but some appeared fully ripe or were in postspawning condition. In September all were partly spawned out.

San Antonio del Mar (31° 06′ N. Lat.). Extensive upwelling and large populations of clams are found at this locality. Those collected in May were all nearly ripe or fully ripe and spawning took place in the aquarium. Of 36 individuals examined in July, one had recently completed spawning and all of the others appeared to be ripe. Spawning was general in the aquarium.[2]

Blanca Bay (29° 06′ N. Lat.). Here also there is cool water and an abundance of large clams. Those examined the first of April showed much variation in the condition of the gonads. Some were in the

[2] Most of the population at this locality died in the early autumn of 1950. The cause has not yet been determined.

early stages of gametogenesis, while others were nearly ripe, fully ripe or partly spawned out. In July all were ripe or partly spawned out.

Thurloe Bay (27° 38′ N. Lat.). Although more than 450 miles south of the Mexican border, the water is cool and conditions are suitable for the production of clams of large size. All of the individuals examined in January were in various stages of gametogenesis but not ripe. Some of those examined in early April were fully ripe or partially spawned, while others were recently spawned out. In July also some were ripe, some were spawned out and others half ripe. It is concluded that the spawning season at favorable localities on the Mexican coast is even less definitely seasonal than it is on the coast of California.

SUMMARY

The fluctuations of the populations have been studied by collecting large samples and returning them to the beach after measurement at monthly intervals for five successive years at La Jolla, California and for two to three years at three other widely separated localities. Many marked individuals were also replanted on the beach and remeasured monthly.

The area investigated at La Jolla covered about 2000 square meters of a beach legally protected from human interference. The constituent year-classes in the population varied considerably from year to year due to differences in the initial set of young clams and the subsequent mortality. It is estimated that an average of three young clams arrived on each square meter each year, but the annual mortality has been from 67 to 75% for each year-class. Of the average annual set of approximately 6000, only about 2000, 700, 170 and 50, respectively, have remained at the end of the first to fourth years. Less than one per cent of the population survived for four years and clams of the legal length of 127 mm were usually found only in deeper, cooler water.

At the other localities investigated, Sunset Beach, Hueneme and Pismo Beach, conditions are more favorable, growth is more rapid and large crops of legal size are produced annually. Many individuals reach an age of seven to twelve years or more. Nevertheless, the mortality rate for each year-class at Pismo Beach, in part due to human agencies, has been estimated as 55, 45, 29, 34, 52, 68 and 72%, respectively, from the first to seventh years.

The populations at Pismo Beach enumerated by the California Bureau of Marine Fisheries in November of 19 years between 1927 and 1949 indicated that an average of 50% of those not more than four years of age belonged to the first year-class and 23, 13 and 14%, respectively, to the second, third and fourth year-classes. Wide

fluctuations were found. In some years only 0 to 10% of the population belonged to the first year-class, while in other years this year-class comprised 60 to 80% of the population.

The most productive areas, both on the Californian and Mexican coasts, are generally those with extensive upwelling of cool oceanic water, bringing with it the inorganic nutrients essential for the growth of the phytoplankton and indirectly for the other organisms and detritus on which the nutrition of the clam depends.

The annual increment in length averages 21 to 25 mm the first and second years of life and somewhat less thereafter. The length of 127 mm, which is the minimum legal size, is reached in five to eight years. The principal spawning season is June to December, although a small proportion of the population has apparently ripe sexual products at any season of the year.

LITERATURE CITED

Aplin, J. A.
1947. Pismo clam increase. Calif. Fish and Game, *33:* 129–131.

Clark, F. N.
1932. The present status of the Pismo clam, *Tivela stultorum.* Calif. Fish and Game, *18:* 170–180.

Coe, W. R.
1947. Nutrition, growth and sexuality of the Pismo clam (Tivela stultorum). J. exp. Zool., *104:* 1–24.
1948. Nutrition, environmental conditions, and growth of marine bivalve mollusks. J. Mar. Res., *7:* 586–601.

Fitch, J. E.[2]
1950. The Pismo clam. Calif. Fish and Game, *36:* 285–312.

Herrington, W. C.
1930. The Pismo clam; further studies of its life history and depletion. Fish Bull., Sacramento, *18:* 1–67.

Roedel, P. M.
1939. The Pismo clam in 1938. Calif. Fish and Game, *25:* 177–181.

Weymouth, F. W.
1923. The life-history and growth of the Pismo clam. Fish Bull., Sacramento, *7:* 1–120.

[2] See for additional references.

THE EFFECT OF FREEZING ON THE SULFATE/CHLORINITY RATIO OF SEA WATER[1]

By

GEORGE J. LEWIS, JR. with THOMAS G. THOMPSON

Oceanographic Laboratories
University of Washington
Seattle, Washington

ABSTRACT

A special refrigeration apparatus was constructed to simulate freezing of sea water under natural conditions. Ice thus obtained, as well as the residual waters, were studied to ascertain the effect of freezing upon the sulfate/chlorinity ratio. This ratio was found to be greater for salts retained by the ice than for the original water. An equivalent decrease in the ratio occurred for the residual water. The ratio in the ices varied considerably and was a function of the rate of formation of ice and the temperatures of exposure. Maximum ratios were obtained at − 8° C and − 45° C. Minimum ratios were obtained at about − 25° C.

The ratio, sulfate/chlorinity, was investigated extensively by Thompson, et al. (7). An average value of 0.1395 was obtained when the concentrations of the sulfate ions were calculated as grams per kilogram of sea water. The values secured on most of the samples were within ± 0.0004 of the average, but a few showed deviations greater than the experimental errors of the methods used for analysis. Data reported by Thompson, et al. (8) give varying ratios, which, in many cases, may be attributed to differences in the methods employed. However, a few of the deviations of the ratio indicate that conditions do exist which may tend to affect the constancy of the sulfate/chlorinity ratio.

The work of Ringer (4, 6) indicated that a considerable increase in the sulfate/chlorinity ratio might occur in sea ice as the result of freezing. He noted that sea water first began to freeze at about − 1.8° C and that further cooling resulted in the initial precipitation of $Na_2SO_4 \cdot 10H_2O$ at − 8.2° C. This decahydrate continued to crystallize with decreasing temperature until, at − 20° C, less than one-tenth of the original sulfate remained in solution. At − 23° C $NaCl \cdot 2H_2O$ began to crystallize, and it continued to form with decreasing temperature to − 53° C. The laboratory conditions of Ringer were decidedly different from those occurring naturally and thus his results are not generally accepted as indicative of sea ice (6).

Wiese (9), on the Russian Sedoff Expedition to Franz Joseph's Land in 1929, found an increase in the ratio with thickness for ice

[1] This work was partly supported by Office of Naval Research contract (no. N8ONR–520/III) with the University of Washington.

formed the previous winter, and he reported a maximum increase of 7% at 97 cm. Six samples of ice which had aged for several years gave a mean value for the ratio that was nearly four times as great as the normal value for sea water; however, this ice was nearly free of salt, the salinity being only 0.15‰.

Repa (3) reported a selective adsorption of sulfate ions by ice from solutions containing both sulfate and chloride ions. He exposed distilled water ice to solutions containing known amounts of sulfate and chloride.

Pettersson (2) reported an increase in the sulfate/chlorinity ratio in natural sea ice.

The data of Sverdrup (5) and Malmgren (1) appear to contradict the results cited above. Their conclusions, based on investigations of natural ice, were made during the Maud Expedition. However, no direct determination of the sulfate ions was made (6).

The studies reported in the present paper were made under laboratory conditions with especially constructed apparatus so that the formation of ice approached more nearly natural conditions.

APPARATUS

A refrigerator was constructed which permitted freezing of samples of sea water from the surface downward. This effect was obtained by building cylindrically shaped wells in the freezing compartment into which the containers of sea water could be placed. The space between the inner wall of the well and the outside of the container was insulated with toweling to prevent freezing around the walls of the container.

Glass battery jars of four liter capacity were used as freezing containers and these were of sufficient strength to withstand the pressure of the sea ice formed. A Frigidaire Meter Miser MM-3 compressor unit, employing F-12 and capable of maintaining temperatures from $-5°$ to $-45°$ C, with a variation of $\pm 3°$ C, was incorporated into the apparatus. The entire unit, with exterior dimensions of 76 x 76 x 170 cm, was portable. Air temperatures of the freezing compartment were taken with a red liquid cold point thermometer having a range from $+20°$ to $-60°$ C.

EXPERIMENTAL PROCEDURE

Sea water samples, taken at various times and locations in the Puget Sound region, were filtered, thoroughly mixed, and about three liters were placed in the battery jar containers. Simultaneously, a sample of the same water was taken and analyzed to determine the sulfate/chlorinity ratio of the original water.

Each sample was exposed to freezing conditions until approximately one-third of the original volume had frozen. The container was then removed from the refrigerator, and the ice and solution were separated and analyzed.

Air temperature readings were taken several times daily to determine the constancy of temperature within the refrigerator. These readings varied within $\pm 3°$ C of the temperature setting on the refrigerator's thermo-regulator.

ANALYSIS OF SAMPLES

The chlorinity and sulfate contents of the original water, ice, and unfrozen solution were determined. The chlorinity was obtained by the Mohr method, using silver nitrate solutions standardized against "normal water" from the Laboratoire Hydrographique in Copenhagen and against recrystallized sodium chloride. Sulfate values were determined by the method used by Thompson, Johnston and Wirth (7). Because of its low salinity content, larger samples of the melted ice were used. Samples taken from the concentrated unfrozen solution were correspondingly smaller. In this way conditions for the precipitation of barium sulfate were made more nearly the same for the original water, unfrozen solution and the melted ice.

The precision of the sulfate analysis of the original waters and of unfrozen solutions was the same as that previously reported (7), an average deviation of $\pm 0.002°/_{oo}$ SO_4. The relative precision for ice samples was slightly less, and experimentally it was found to be 1 part in 500.

EXPERIMENTAL RESULTS AND DISCUSSION

Fourteen samples of sea water were frozen and analyzed for chlorinity and sulfate. The results are tabulated in Table I, and a summary of the data is given in Table II. The sulfate/chlorinity ratios are given for the original sea water samples, the ices and the resulting unfrozen solutions. The absolute increases in the ratio in the ice over those in the original waters have been calculated and tabulated in the column under the heading $\Delta(SO_4/Cl)$. The temperature at which each sample was frozen is given, as well as the time of exposure to freezing conditions.

In Table III are tabulated $\Delta(SO_4/Cl)$, $\Delta SO_4°/_{oo}$, and percent SO_4 increase. These values were averaged from Table I. The difference between the experimentally determined value for sulfate in the ice and the value which would obtain if the sulfate/chlorinity ratio were the same in the ice as in the original water is designated by $\Delta SO_4°/_{oo}$.

TABLE I.—Experimental Results

Sample	Cl°/$_{oo}$	SO_4°/$_{oo}$	SO_4/Cl	$\Delta(SO_4/Cl)$	*Temp.* ° C	*Freezing Period (hours)*
Y Orig	16.48	2.307	0.1400		− 8	158
Ice	4.47_3	0.640_7	0.1432	0.0032		
Soln	21.16	2.952	0.1395			
Z Orig	16.46	2.301	0.1398		− 8	193
Ice	4.30_0	0.614_7	0.1430	0.0032		
Soln	20.20	2.816	0.1394			
P Orig	18.05	2.516	0.1394		− 16	42
Ice	7.23_8	1.019	0.1408	0.0014		
Soln	19.67	2.740	0.1393			
G Orig	17.10	2.387	0.1396		− 25	19
Ice	7.76_4	1.087	0.1400	0.0004		
Soln	19.97	2.776	0.1390			
I Orig	17.11	2.386	0.1395			24
Ice	7.06_7	0.989_6	0.1400	0.0005	− 25	
Soln	20.34	2.818	0.1385			
R Orig	16.64	2.325	0.1397		− 25	41
Ice	6.28_6	0.882_0	0.1403	0.0006		
Soln	21.95	3.053	0.1391			
U Orig	15.81	2.205	0.1395		− 25	32
Ice	6.36_1	0.888_9	0.1397	0.0002		
Soln	20.53	2.870	0.1398			
T Orig	17.67	2.475	0.1401		− 27	41
Ice	7.59_1	1.068	0.1407	0.0006		
Soln						
W Orig	16.44	2.305	0.1402		− 28	24
Ice	6.84_4	0.963_0	0.1407	0.0005		
Soln	24.60	3.440	0.1398			
V Orig	18.16	2.540	0.1399		− 40	20
Ice	6.66_7	0.939_8	0.1410	0.0011		
Soln	22.33	3.114	0.1395			
X Orig	16.43	2.306	0.1404		− 40	18
Ice	6.82_9	0.960_0	0.1406	0.0002		
Soln	21.56	3.010	0.1396			
J Orig	16.87	2.353	0.1395		− 45	19
Ice	8.64_2	1.231	0.1424	0.0029		
Soln	21.60	2.994	0.1386			
L Orig	16.03	2.227	0.1389		− 45	16
Ice	8.47_4	1.206	0.1423	0.0034		
Soln	20.66	2.850	0.1380			
M Orig	15.96	2.229	0.1397		− 45	16
Ice	7.04_2	1.001	0.1422	0.0025		
Soln	20.39	2.814	0.1380			

TABLE II.—Average of All Results Shown in Table I

	Cl°/₀₀	SO_4°/₀₀	SO_4/Cl	Δ(SO_4/Cl)
Orig.	16.80	2.347	0.1397	
Ice	6.82₇	0.963	0.1412	0.0015
Soln.	21.15	2.942	0.1391	

TABLE III.—Increases in SO_4/Cl and SO_4°/₀₀, and Percent Increase in Concentration of Sulfate Ion in Ice Frozen at Various Temperatures (Mean Values Taken from Table I)

Temperature ° C	Δ(SO_4/Cl)	ΔSO_4°/₀₀	*Percent* SO_4 *Increase*
− 8°	0.0032	0.015	2.39
− 16°	0.0014	0.010	0.98
− 26°	0.0005	0.004	0.36
− 40°	0.0007	0.004	0.42
− 45°	0.0029	0.024	2.04

The value of SO_4°/₀₀ which would have occurred if there had been no selective retention of sulfate was obtained by multiplying the chlorinity of the ice by the sulfate/chlorinity ratio of the original water. Percent SO_4 increase was secured by dividing ΔSO_4°/₀₀ by the experimental SO_4°/₀₀ for the ice. Δ(SO_4/Cl) versus temperature is plotted in Fig. 1.

Fig. 1 shows that the greatest increases in the sulfate/chlorinity ratio occurred in samples frozen at − 8° C and at − 45° C. The large increase at − 8° C might be attributed to selective adsorption of sulfate ions, as suggested by Repa (3) who has reported an increase in adsorbed sulfate with time. Thus, for slowly frozen samples a greater adsorption of sulfate might be expected than for more rapidly frozen samples.

In samples frozen at − 45° C, the marked selective retention of sulfate by the ice was probably due to precipitation of sodium sulfate from pockets of concentrated brine which were temporarily retained by the loose network of ice crystals at the interface between solid and solution. The fact that Ringer found a maximum sulfate/chlorinity ratio in the ice at − 20° C is not contradicted by a maximum with an air temperature of − 45° C, because a large thermal gradient occurred in the ice (the solution never became concentrated enough to be more than about − 2° C), and consequently the brine pockets were probably never much colder than − 20° even in the ice layers which formed at the surface.

Likewise, the minimum between − 8° and − 45° C may be attributed to conditions which were conducive to neither appreciable precipitation of Na_2SO_4 nor selective adsorption of sulfate.

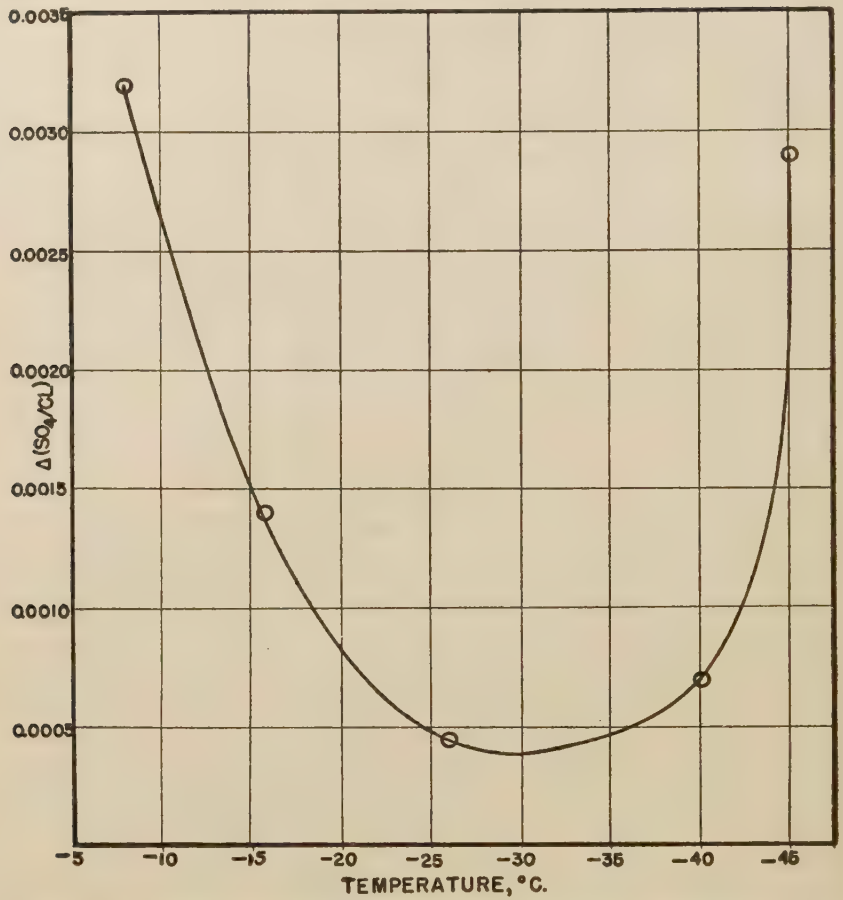

Figure 1.—Increase in the sulfate/chlorinity ratios in ice versus the temperatures at which the samples were frozen. Data from Table III.

CONCLUSIONS

1. An increase in the sulfate/chlorinity ratio occurred in the salts retained by ice as the result of the freezing of sea water.

2. The increase in this ratio varied with the temperature at which the water was frozen.

3. Maximum increases in the sulfate/chlorinity ratio of 0.0032 and 0.0029 were obtained at − 8° and − 45° C respectively.

4. A minimum increase in the sulfate/chlorinity ratio of 0.0004 was obtained for samples frozen at temperatures − 25° to − 28° C.

LITERATURE CITED

1. Malmgren, Finn
1927. On the properties of sea-ice. Sci. Res. Norweg. N. Pol. Exped. "Maud," *1* (5): 1–67. See pp. 4–11.

2. Pettersson, O.
1883. Die Eigenschaften von Wasser und Eis. Vega-Exped. Vetensk. Jakt., *2:* 249–323, as reviewed in Beibl. Ann. Phys., *7:* 834–841.

3. Repa, A. G.
1938. On the chemical adsorption by ice of SO_4'' and Cl' ions. Bull. Far East. Br., Acad. Sci. U. S. S. R., No. 31 (4): 43–47 + Eng. Summary on p. 48.

4. Ringer, W, E,
1906. De veranderingen in samenstelling van zeewater bij het bevriezen. Chem. Weekbl., *3:* 223–249.

5. Sverdrup, H. U.
1929. The waters on the North-Siberian Shelf. Sci. Res. Norweg. N. Pol. Exped. "Maud," *4* (2): 131 + 75 pp. See pp. 119–129.

6. Sverdrup, H. U., M. W. Johnson and R. H. Fleming
1946. The Oceans. Prentice-Hall, Inc., N. Y. 1087 pp. See pp. 216–219.

7. Thompson, T. G., W. R. Johnston and H. E. Wirth
1931. The sulfate-chlorinity ratio in ocean waters. J. Cons. int. Explor. Mer, *6:* 246–251.

8. Thompson, T. G., J. W. Lang and L. Anderson
1927. The sulfate-chlorinity ratio of the waters of the North Pacific. Publ. Puget Sd. Mar (biol.) Sta., *5:* 277–292.

9. Wiese, W.
1930. Zur Kenntnis der Salze des Meereises. Ann. Hydrog., Berl., *58:* 282–286.

NOTE ON THE DYNAMICS OF THE GULF STREAM[1]

By

W. H. MUNK,[2 3] G. W. GROVES[2] AND G. F. CARRIER[4]

ABSTRACT

The nonlinear inertial terms have been neglected in Stommel's and in Munk's theory for the wind-driven ocean circulation. Using a method of successive approximations, the effect of these terms on the mass transport in the Gulf Stream region has been computed under greatly simplifying assumptions. These assumptions involve Reid's model of the vertical density structure, which consists of an exponential decrease in the density upward to the thermocline and a homogeneous upper layer. Assuming first a constant depth of thermocline and a north-south boundary, the principal modification is a displacement downstream by about 7° latitude of the region of maximum currents. The displacement is smaller in the case of a coastline whose orientation deviates from a north-south direction. Assuming next a variation in the depth of thermocline across the stream, this asymmetry of the mass transport circulation relative to the wind circulation is reduced. It is also shown that the density model specifies a relation between the vertically integrated transport and the surface transport, according to which the width of the "cold wall" at the surface is only 40% of that of the integrated transport. Two observed features which could not be accounted for by the linear theory, the countercurrent inshore and the continued sharpness of the Gulf Stream's western boundary long after it has left the American east coast, are apparently not contained in the higher order solutions.

INTRODUCTION

The narrow fast currents that flow along the western boundaries of the oceans are among the most striking oceanographic phenomena. The outstanding examples are the Kuroshio current off the coast of Japan and the Gulf Stream system off the American east coast. During the last few years Iselin and Fuglister (1948) and Von Arx (1950) have made detailed surveys of the Gulf Stream with new instruments and techniques, among them continuous temperature and current recorders and radio aids to navigation. These measurements have only served to emphasize the great speed of the Gulf Stream and the sharpness of its western boundary. This sharp definition of the current, which prompted Benjamin Franklin to call it a great river in

[1] Contribution from the Scripps Institution of Oceanography, New Series No. 496. This work represents research carried out for the Office of Naval Research, Navy Department.

[2] Scripps Institution of Oceanography, University of California.

[3] Institute of Geophysics, University of California.

[4] Department of Applied Mathematics, Brown University.

the sea, is perhaps its most striking characteristic. Any adequate theory, and there have been many, must account for it.

Unfortunately there are two theories, both of which explain, though for different reasons, the existence of such intense and well defined currents. The earlier one is Rossby's (1936) "wake stream" or "jet stream" theory, which represents one of his several remarkable attempts to adapt results in fluid mechanics to meteorology and physical oceanography. The Gulf Stream is interpreted as "a current moving under its own momentum and produced by discharging water into the basin through a 'jet'" (the Straits of Florida). The other theory is that of Stommel (1948), which explains the westward intensification of ocean currents as the result of the earth's rotation on the wind-driven ocean circulation. The theory has been extended by Munk (1950), and for reasons discussed in Munk's paper it will be referred to as the "planetary vorticity" theory.

Both theories have attractive features. The wake stream theory accounts for the increase downstream in width and mass transport of the Gulf Stream as well as a countercurrent on the inshore side of the Gulf Stream.[5] The planetary vorticity theory leads to the right order of magnitude for the mass transport of the Gulf Stream, and it accounts for a countercurrent on the offshore side. One is therefore tempted to combine the two theories into a unified dynamic picture of the Gulf Stream.

The fundamental difference appears to be that in Stommel's and in Munk's linear theory the inertial terms in the equations of motion have been neglected whereas in Rossby's theory these terms play a predominant role. Munk estimates the magnitude of these terms *a posteriori* and finds them to be small "except along the inshore edge of the western current," where he expects his conclusions to be modified in the sense prescribed by Rossby. The procedure here will be to consider Munk's solution to the linear theory as a zero approximation and to introduce the inertial terms into the first and second order approximations.

The mathematics soon becomes so involved that we have found it essential to check each step by independent calculations. Only the outline of the procedure is sketched here. We suggest that the reader confine his attention to the discussion of the somewhat meager results from our tedious calculations.

[5] The first mention of a countercurrent in the slope water was made in 1590 by John White, who remarked that in order to stay within the Gulf Stream one had to stand far out to sea, because along the coast there were "eddy currents setting to the south and southwest."

THE EQUATIONS OF MOTION

The notation follows Munk (1950); equations from this paper will be referred to by the letter A. The inertial terms appear on the left sides of equations A1, A4, A6 in the following forms:[6]

$$\rho \mathbf{v} \cdot \nabla \mathbf{v}\,, \quad \int_{-\infty}^{h} \rho \mathbf{v} \cdot \nabla \mathbf{v} dz\,, \quad -\nabla \times \int_{-\infty}^{h} \rho \mathbf{v} \cdot \nabla \mathbf{v} dz\,.$$

In the linear theory it was found possible to write all equations in terms of vertically integrated functions without having to specify the manner in which density varies with depth. This is no longer possible if the quadratic terms are to be considered.

Reid (1948) has introduced a simple model for the density distribution. Let the z-axis be directed upwards from a level surface just beneath the sea surface, and let h designate the elevation of the sea surface and H the distance beneath the level reference surface to which a homogeneous upper layer of density ρ_0 extends. Beneath the homogeneous layer, Reid assumes an exponential distribution

$$\rho = \rho_\infty - \Delta\rho e^{1+z/H},$$

where $\Delta\rho = \rho_\infty - \rho_0$, and ρ_∞ is the density at great depth ($z = -\infty$).

The horizontal pressure gradient vanishes at great depth, i. e. $\int_{-\infty}^{h} \rho\, dz =$ constant, which yields

$$\frac{h}{H} = \frac{2\Delta\rho}{\rho_0}, \tag{1}$$

provided the reference level is properly selected.

The pressure gradient in the x-direction is then given for the upper layer by

$$\frac{\partial p_0}{\partial x} = g\rho_0 \frac{\partial h}{\partial x} \tag{2}$$

and for the lower layer by

$$\frac{\partial p}{\partial x} = \frac{1}{2} g\rho_0 e^{1+z/H} (1 - z/H) \frac{\partial h}{\partial x}, \tag{3}$$

where use has been made of (1). Similar expressions are valid for $\partial p/\partial y$. According to the geostrophic law, the pressure gradients are proportional to the horizontal velocity components. If $\mathbf{v}_0$ denotes the velocity vector in the upper layer, then

[6] Here h and $-\infty$ replace z_0 and $-h$, respectively, in the original notation, without any essential change in meaning.

$$\frac{1}{2}\,\mathbf{v}_0\, e^{1+z/H}(1 - z/H)$$

is the corresponding velocity at depths beneath the homogeneous layer. It follows that

$$\int_{-\infty}^{h} \bar{\rho}\mathbf{v} \cdot \nabla\mathbf{v}dz = \frac{29}{16}\,\bar{\rho}H\,(\mathbf{v}_0 \cdot \nabla)\,\mathbf{v}_0 + \frac{29}{32}\,\bar{\rho}\mathbf{v}_0\,(\mathbf{v}_0 \cdot \nabla)\,H\,.$$

The second term is negligible since H is nearly constant along a stream line. The first term can be combined with

$$\boldsymbol{M} \equiv \int_{-\infty}^{h} \rho\mathbf{v}dz = \frac{5}{2}\,\bar{\rho}H\mathbf{v}_0 \tag{4}$$

to yield

$$\int_{-\infty}^{h} \bar{\rho}\mathbf{v}\cdot\nabla\mathbf{v}dz = c\boldsymbol{M}\cdot\nabla\boldsymbol{M}\,, \tag{5}$$

where

$$c = 29/100\bar{\rho}H\,, \tag{6}$$

provided variations in density are small compared to the mean density $\bar{\rho}$.

The equation of mass transport A6 then becomes

$$\left(A\nabla^4 - \beta\frac{\partial}{\partial x}\right)\psi + \mathrm{curl}_z\,\tau = c\,\mathrm{curl}_z\,(\boldsymbol{M}\cdot\nabla\boldsymbol{M}) = c\,(\boldsymbol{M}\cdot\nabla)\,\nabla^2\psi\,, \tag{7}$$

where

$$\boldsymbol{M} = \boldsymbol{k} \times \nabla\psi$$

and curl_z designates the vertical component of the vector operator. The term on the right side of equation (7) is essentially the advection of vorticity and represents the inertial effect.

For a wind system we set

$$\tau_x = -\,\Gamma\cos ny\,, \quad \tau_y = 0\,,$$

giving maximum easterlies at $y = 0$ and maximum westerlies at $y = \pi/n$.

THE CASE OF NORTH-SOUTH BOUNDARIES AND CONSTANT DEPTH OF THERMOCLINE

For this case c is a constant. It is convenient to adopt the following nondimensional co-ordinate system:

$$x' = kx \qquad \psi' = \frac{\beta}{\Gamma n r}\psi$$

$$y' = ky \qquad M' = \frac{\beta}{k\Gamma n r} M \tag{8}$$

$$r' = kr \qquad \lambda = \frac{n^4 r \Gamma c}{4\beta^2\gamma^2},$$

$$y'' = ny$$

where

$$k^3 = \beta/A\,, \quad \gamma = n/k\,. \tag{9}$$

It follows that

$$\frac{\partial}{\partial x} = k\frac{\partial}{\partial x'}\,, \qquad \frac{\partial}{\partial y} = k\frac{\partial}{\partial y'}\,, \qquad \nabla^4 = k^4\nabla'^4\,, \tag{10}$$

so that the differential equation becomes

$$\left(\nabla'^4 - \frac{\partial}{\partial x'}\right)\psi' = \frac{1}{r'}\sin y'' + 4\gamma^{-1}\lambda\,\mathrm{curl}_z\,(\boldsymbol{M}'\cdot\nabla'\boldsymbol{M}')\,, \tag{11}$$

$$\boldsymbol{M}' = \boldsymbol{k}\times\nabla'\psi'\,. \tag{12}$$

The boundary conditions are

$$\psi' = 0\,, \qquad \frac{\partial\psi'}{\partial x'} = 0\,, \tag{13}$$

at the western boundary ($x' = 0$) and eastern boundary ($x' = r'$); the latter can be replaced by $x' = \infty$ as long as we confine our attention to conditions near the western boundary.

Successive Approximations. The first term on the right-hand side of equation (11) represents the driving force of the wind, the second term incorporates the effect of the neglected inertial terms. The relative importance of these inertial terms depends on the value of λ, and it seems reasonable to expand the solution in the following power series:

$$\psi' = \psi_0' + \lambda\psi_1' + \lambda^2\psi_2' + \ldots \tag{14}$$

We shall show later that the value of λ is about 0.3 so that the series converges fairly rapidly. Substituting (14) into equations (11) and (12) and equating equal powers of λ gives

$$\left(\nabla'^4 - \frac{\partial}{\partial x'}\right)\psi_0' = \frac{1}{r'}\sin y''\,, \tag{11.0}$$

$$\left(\nabla'^4 - \frac{\partial}{\partial x'}\right)\psi_1' = 4\gamma^{-1}\,\mathrm{curl}_z\,(\boldsymbol{M}_0'\cdot\nabla'\boldsymbol{M}_0')\,, \tag{11.1}$$

$$\left(\nabla'^4 - \frac{\partial}{\partial x'}\right)\psi_2' = 4\gamma^{-1}\,\mathrm{curl}_z\,(\boldsymbol{M}_0'\cdot\nabla'\boldsymbol{M}_1' + \boldsymbol{M}_1'\cdot\nabla'\boldsymbol{M}_0')\,, \qquad (11.2)$$

and so forth. Equation (12) holds for each order, that is,

$$\boldsymbol{M}_i' = \boldsymbol{k}\times\nabla'\psi_i' \qquad i = 0, 1, 2, \ldots \qquad (12i)$$

The Zero Order. To the zero approximation the inertial terms are neglected and the solution to (11.0) becomes (Munk and Carrier, 1950)

$$\psi_0' = X_0 \sin y'', \qquad (15.0)$$

where

$$X_0 = 1 + \frac{i\sqrt{3}\omega}{3}\,e^{\omega^2 x'} - \frac{i\sqrt{3}\omega^2}{3}\,e^{\omega x'} - \frac{x'}{r'}\,, \qquad (16.0)$$

and

$$\omega = -\frac{1}{2} + \frac{i\sqrt{3}}{2}\,, \qquad \omega^2 = -\frac{1}{2} - \frac{i\sqrt{3}}{2}\,, \qquad \omega^3 = 1$$

are the cube roots of one. The last term in (16.0) plays a negligible role in the western boundary zone of a wide ocean.

The First Order. The computation is very cumbersome and hence only the major steps will be outlined here. The right side of equation (11.1) is now a known function of x', since it can be found from equations (15.0) and (16.0). It reduces to the form

$$2F_1 \sin 2y'', \qquad (17.1)$$

where

$$F_1 = \frac{\partial X_0}{\partial x'}\,\frac{\partial^2 X_0}{\partial x'^2} - X_0\frac{\partial^3 X_0}{\partial x'^3} \qquad (18.1)$$

$$= -e^{-x'} - \frac{i\sqrt{3}\omega}{3}\,e^{\omega^2 x'} + \frac{i\sqrt{3}\omega^2}{3}\,e^{\omega x'}\,. \qquad (19.1)$$

The particular and homogeneous integrals of (11.1) are respectively

$$\psi_1'^p = \left[-e^{-x'} - \frac{2i\sqrt{3}\omega}{9}\,x'e^{\omega^2 x'} + \frac{2i\sqrt{3}\omega^2}{9}\,x'e^{\omega x'}\right]\sin 2y''\,, \qquad (20.1)$$

$$\psi_1'^h = [a_1 e^{\omega^2 x'} + \bar{a}_1 e^{\omega x'}]\sin 2y''. \qquad (21.1)$$

The constants a_1 and $\bar{a}_1$ are determined by subjecting the complete solution $\psi_1' = \psi_1'^p + \psi_1'^h$ to the boundary conditions (13):

$$a_1 = \frac{1}{2} - \frac{7i\sqrt{3}}{18}\,, \qquad \bar{a}_1 = \frac{1}{2} + \frac{7i\sqrt{3}}{18}\,. \qquad (22.1)$$

The solution is

$$\psi_1' = X_1 \sin 2y'', \tag{23.1}$$

$$X_1 = -e^{-x'} + (m_1 + in_1)e^{\omega^2 x'} + (m_1 - in_1)e^{\omega x'}, \tag{24.1}$$

where

$$m_1 = \frac{1}{2} + \frac{1}{3}x', \qquad n_1 = -\frac{7\sqrt{3}}{18} + \frac{\sqrt{3}}{9}x'.$$

The Second Order. Substituting the first order solution (23.1) into the right side of the second order equation (11.2) gives

$$(2F_2 - 4G_2)\sin y'' + (2F_2 + 4G_2)\sin 3y'', \tag{17.2}$$

where

$$F_2 = \frac{\partial^2 X_0}{\partial x'^2}\frac{\partial X_1}{\partial x'} - X_0\frac{\partial^3 X_1}{\partial x'^3} \tag{18.2a}$$

$$\left.\begin{aligned} = \left(\frac{2}{3}x' - \frac{19}{9}\right)e^{-x'} - (m_2 - in_2)e^{\omega^2 x'} - (m_2 + in_2)e^{\omega x'} \\ - \frac{4}{9}e^{2\omega^2 x'} - \frac{4}{9}e^{2\omega x'} + e^{(\omega^2-1)x'} + e^{(\omega-1)x'}; \end{aligned}\right\} \tag{19.2a}$$

$$G_2 = \frac{\partial X_0}{\partial x'}\frac{\partial^2 X_1}{\partial x'^2} - \frac{\partial^3 X_0}{\partial x'^3}X_1 \tag{18.2b}$$

$$\left.\begin{aligned} = \left(\frac{2}{3}x' + \frac{1}{9}\right)e^{-x'} + \frac{4}{9}e^{2\omega^2 x'} + \frac{4}{9}e^{2\omega x'} \\ + \omega^2 e^{(\omega^2-1)x'} + \omega e^{(\omega-1)x'}; \end{aligned}\right\} \tag{19.2b}$$

and

$$m_2 = -\frac{1}{2} + \frac{x'}{3}, \qquad n_2 = \frac{\sqrt{3}}{18} - \frac{\sqrt{3}x'}{9}.$$

The particular integral equals

$$\left.\begin{aligned} \psi_2'^p = \left\{\left(-\frac{2}{3}x' - 4\right)e^{-x'} + (m' + in')\,e^{\omega^2 x'} + (m' - in')\,e^{\omega x'}\right. \\ - \frac{4\omega}{21}e^{2\omega^2 x'} - \frac{4\omega^2}{21}e^{2\omega x'} + \frac{1}{21}(13\omega^2 + 11)\,e^{(\omega^2-1)x'} \\ \left. + \frac{1}{21}(13\omega + 11)\,e^{(\omega-1)x'}\right\}\sin y'' + \left\{\left(2x' + \frac{28}{9}\right)e^{-x'}\right. \\ + (m' + in')\,e^{\omega^2 x'} + (m' - in')\,e^{\omega x'} + \frac{4\omega}{63}e^{2\omega^2 x'} + \frac{4\omega^2}{63}e^{2\omega x'} \\ \left. + \frac{1}{7}(\omega - 2)\,e^{(\omega^2-1)x'} + \frac{1}{7}(\omega^2 - 2)\,e^{(\omega-1)x'}\right\}\sin 3y'', \end{aligned}\right\} \tag{20.2}$$

where

$$m' = -\frac{1}{9}x'^2 - \frac{1}{9}x', \qquad n' = -\frac{\sqrt{3}}{27}x'^2 + \frac{5\sqrt{3}}{27}x'.$$

The homogeneous solution is

$$\psi_2'^h = [a_2 e^{\omega 2x'} + \bar{a}_2 e^{\omega x'}] \sin y'' + [b_2 e^{\omega 2x'} + \bar{b}_2 e^{\omega x'}] \sin 3y'', \quad (21.2)$$

where, according to the boundary conditions,

$$a_2 = \frac{71}{42} + \frac{115i\sqrt{3}}{378}, \qquad b_2 = -\frac{7}{6} - \frac{173i\sqrt{3}}{378},$$

and $\bar{a}_2$, $\bar{b}_2$ are the corresponding conjugates. The complete second order solution is found by adding $\psi_2'^p$ to $\psi_2'^h$.

THE CASE OF THE INCLINED BOUNDARY

Munk and Carrier (1950) have treated the case of a triangular ocean, with a western boundary inclined by an angle θ from a north-south direction. For an application of the foregoing results to the Gulf Stream, whose over-all direction along the western boundary of the Atlantic is more nearly eastward than northward, it is necessary to see what modifications are introduced by such an inclination.

It will be convenient to introduce the parameter

$$p^3 = \cos^4\theta \quad (25)$$

and to transform to the co-ordinate system

$$\xi = px' - py' \tan\theta, \qquad \zeta = y'. \quad (26)$$

Here ξ represents the (nondimensional) distance from the inclined western boundary. Then

$$\begin{aligned} \frac{\partial}{\partial x'} &= p\frac{\partial}{\partial \xi}, & \frac{\partial}{\partial y'} &= -p\tan\theta\frac{\partial}{\partial \xi}, \\ \nabla' &= \boldsymbol{q}\frac{\partial}{\partial s} + \boldsymbol{j}\frac{\partial}{\partial \zeta}, & \nabla'^4 &= p\frac{\partial^4}{\partial \xi^4}, \end{aligned} \quad (27)$$

where $\boldsymbol{q} = p(\boldsymbol{i} - \boldsymbol{j}\tan\theta)$. The approximations involved are discussed in Munk and Carrier (1950). It follows that

$$\operatorname{curl}_z (\boldsymbol{M}' \cdot \nabla' \boldsymbol{M}') = p^{3/2} (\psi_\xi' \psi_{\xi\xi\zeta}' - \psi_\zeta' \psi_{\xi\xi\xi}'),$$

whereas previously

$$\operatorname{curl}_z (\boldsymbol{M}' \cdot \nabla' \boldsymbol{M}') = \psi_{x'}' \psi_{x'x'y'}' - \psi_{y'}' \psi_{x'x'x'}'.$$

Making the appropriate substitutions, the differential equation (11) becomes

$$\left(\nabla'^4 - \frac{\partial}{\partial \xi}\right)\psi' = \frac{1}{pr'}\sin y'' + 4\gamma^{-1}\sqrt{p}\,\lambda\,\mathrm{curl}_z\,(\boldsymbol{M}'\cdot\nabla'\boldsymbol{M}')\,, \quad (28)$$

with the understanding that all operations now involve ordinary Cartesian operators with respect to ξ and ζ, and not those defined in (27). Thus in equation (28)

$$\nabla'^4 = \frac{\partial^4}{\partial\xi^4} + 2\frac{\partial^4}{\partial\xi^2\partial\zeta^2} + \frac{\partial^4}{\partial\zeta^4}\,, \qquad \boldsymbol{M}' = \boldsymbol{k}\times\left(\boldsymbol{i}\frac{\partial\psi'}{\partial\xi} + \boldsymbol{j}\frac{\partial\psi'}{\partial\zeta}\right),$$

etc. Equations (28) and (11) are equivalent and the previously derived solutions apply, provided we write

for

$\sqrt{p}\,\lambda$,	pr',	ξ
λ,	r',	x'.

(29)

For $\theta = 0$, $p = 1$, the solution reduces again to the case of north-south boundary.

DISCUSSION OF SOLUTION

The solution in real form for the north-south boundaries is then

$$\psi' = X_0\sin y'' + \lambda X_1\sin 2y'' + \lambda^2\,(X_2{}^a\sin y'' + X_2{}^b\sin 3y'') + \ldots \quad (22)$$

where

$$X_0 = 1 - \left[\cos\frac{\sqrt{3}}{2}x' + \frac{\sqrt{3}}{3}\sin\frac{\sqrt{3}}{2}x'\right]e^{-\frac{1}{2}x'}\,, \quad (23.0)$$

$$X_1 = \left[\left(1+\frac{2}{3}x'\right)\cos\frac{\sqrt{3}}{2}x' + \left(-\frac{7\sqrt{3}}{9} + \frac{2\sqrt{3}}{9}x'\right)\sin\frac{\sqrt{3}}{2}x'\right]e^{-\frac{1}{2}x'} - e^{-x'}\,, \quad (23.1)$$

$$X_2{}^a = \left[\left(-\frac{2}{9}x'^2 - \frac{2}{9}x' + \frac{71}{21}\right)\cos\frac{\sqrt{3}}{2}x' + \left(-\frac{2\sqrt{3}}{27}x'^2 + \frac{10\sqrt{3}}{27} + \frac{115\sqrt{3}}{189}\right)\sin\frac{\sqrt{3}}{2}x'\right]e^{-\frac{1}{2}x'} + \left[\frac{4}{21}\cos\sqrt{3}x' - \frac{4\sqrt{3}}{21}\sin\sqrt{3}x' - \frac{2}{3}x' - 4\right]e^{-x'} + \left[\frac{3}{7}\cos\frac{\sqrt{3}}{2}x' - \frac{13\sqrt{3}}{21}\sin\frac{\sqrt{3}}{2}x'\right]e^{-\frac{3}{2}x'} \quad (23.2a)$$

$$X_2{}^b = \left[\left(-\frac{2}{9}x'^2 - \frac{2}{9}x' - \frac{7}{3}\right)\cos\frac{\sqrt{3}}{2}x' + \left(-\frac{2\sqrt{3}}{27}x'^2 + \frac{10\sqrt{3}}{27}x' - \frac{173\sqrt{3}}{189}\right)\sin\frac{\sqrt{3}}{2}x'\right]e^{-\frac{1}{2}x'} + \left[-\frac{4}{63}\cos\sqrt{3}\,x' + \frac{4\sqrt{3}}{63}\sin\sqrt{3}x' + 2x' + \frac{28}{9}\right]e^{-x'} + \left[-\frac{5}{7}\cos\frac{\sqrt{3}}{2}x' + \frac{\sqrt{3}}{7}\sin\frac{\sqrt{3}}{2}x'\right]e^{-\frac{3}{2}x'} \quad . \quad (23.2b)$$

We shall first discuss this solution and then point out the modifications introduced by an inclination of the boundary relative to the north-south direction.

The four functions X of the zero, first and second order approximations are plotted in Fig. 1. The streamlines of the zero, first and second order solution are plotted separately in Fig. 2. The three parts of the figure must be combined, each part being weighted according to the value of λ. We shall leave aside for the present the question of the value of λ and consider separately the patterns corresponding to the various orders. Allowance must be made for the exaggeration of the west-east scale relative to the north-south scale by a factor of $10\pi/96\gamma$, or about 8. Thus the north-flowing currents are much more intense than they appear on the figures.

The left part of Fig. 2 gives essentially the solution discussed in Munk (1950). The first order solution (Fig. 2, center) reveals four vortices with a saddle point at their center. The eastern vortex pair is of relatively small interest, as the neglect of the last term in equation (16.0) introduces errors in the Sargasso Sea area. Of the western vortex pair, the southern vortex weakens the Gulf Stream near shore, the northern vortex strengthens it. The second order solution (Fig. 2, right) reveals three vortices.

The net modification introduced by the first and second order terms can be seen qualitatively to consist of strengthening the current in northern latitudes where all of the terms add and of weakening the current in the central portion. As a result the circulation pattern is displaced northward. This result could have been anticipated, as one would naturally expect the effect of inertia to reduce the current strength in a region of acceleration and to increase it in a region of deceleration.[7]

[7] More precisely, to diminish vorticity in regions where the vorticity increases downstream, and vice versa.

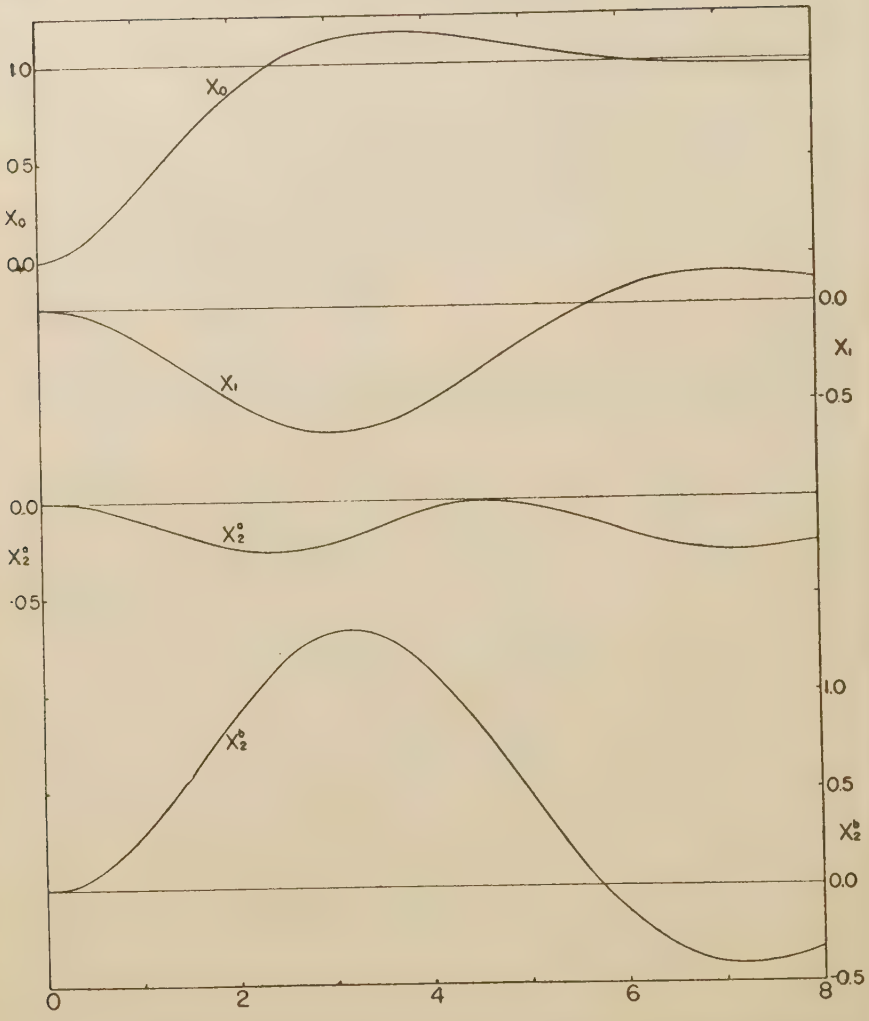

Figure 1. The finctions X of the zero, first and second orders, plotted against the non-dimensional distance x' from the western boundary.

The quantitative extent of these modifications depends upon the numerical value of λ. Setting $\pi/n = 35°$ latitude, $r'' = 6$, $\Gamma = 0.65$ dynes cm^{-2}, $\beta = 2 \times 10^{-13}$ cm^{-1} sec^{-1}, $\gamma = 0.04$, $\bar{\rho} = 1.025$ g cm^{-3} gives [equations (6) and (8)]

$$\lambda = 2784/H\,, \tag{30}$$

Figure 2. Streamlines of mass transport. The nondimensional west-east scale is exaggerated relative to the north-south scale by a factor of about 8, so that the currents are much more intense than they appear in the figure. Left: zero order solution ψ_0'; center: first order solution ψ_1'; right: second order solution ψ_2'.

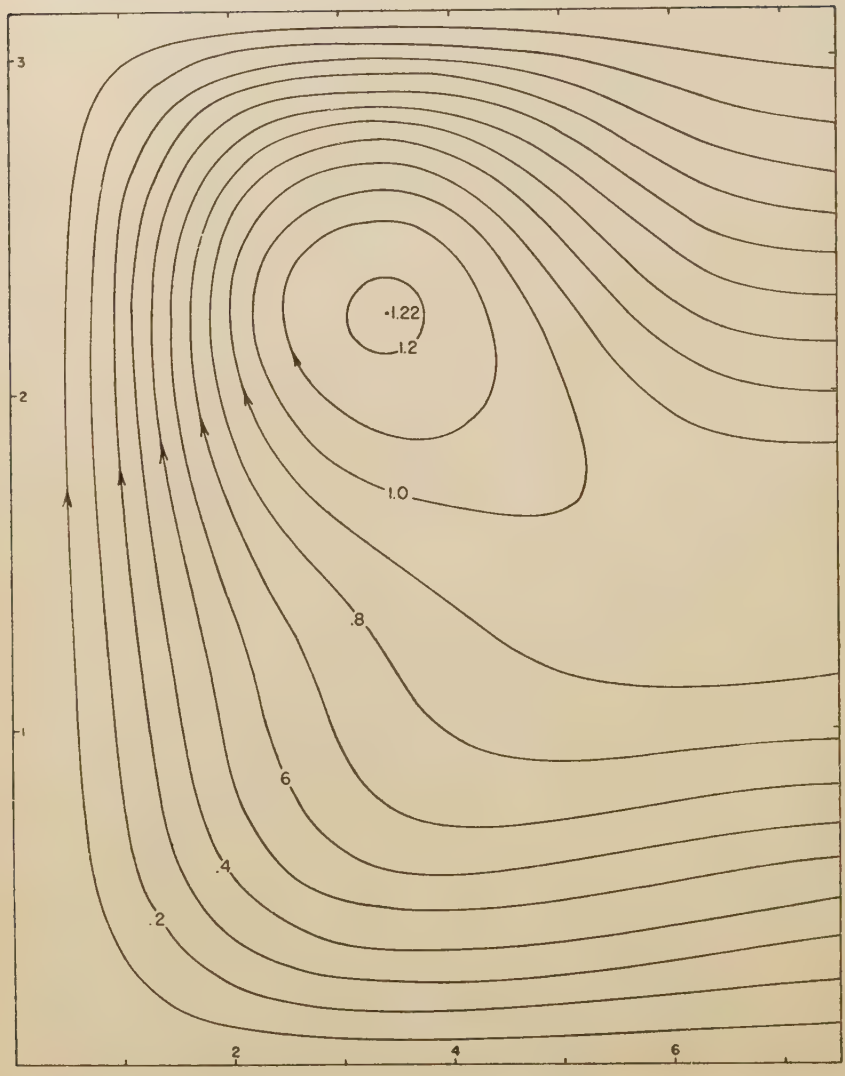

Figure 3. Streamlines of mass transport, ψ', for the sum of the zero, first, and second order solutions, assuming $\lambda = 0.4$.

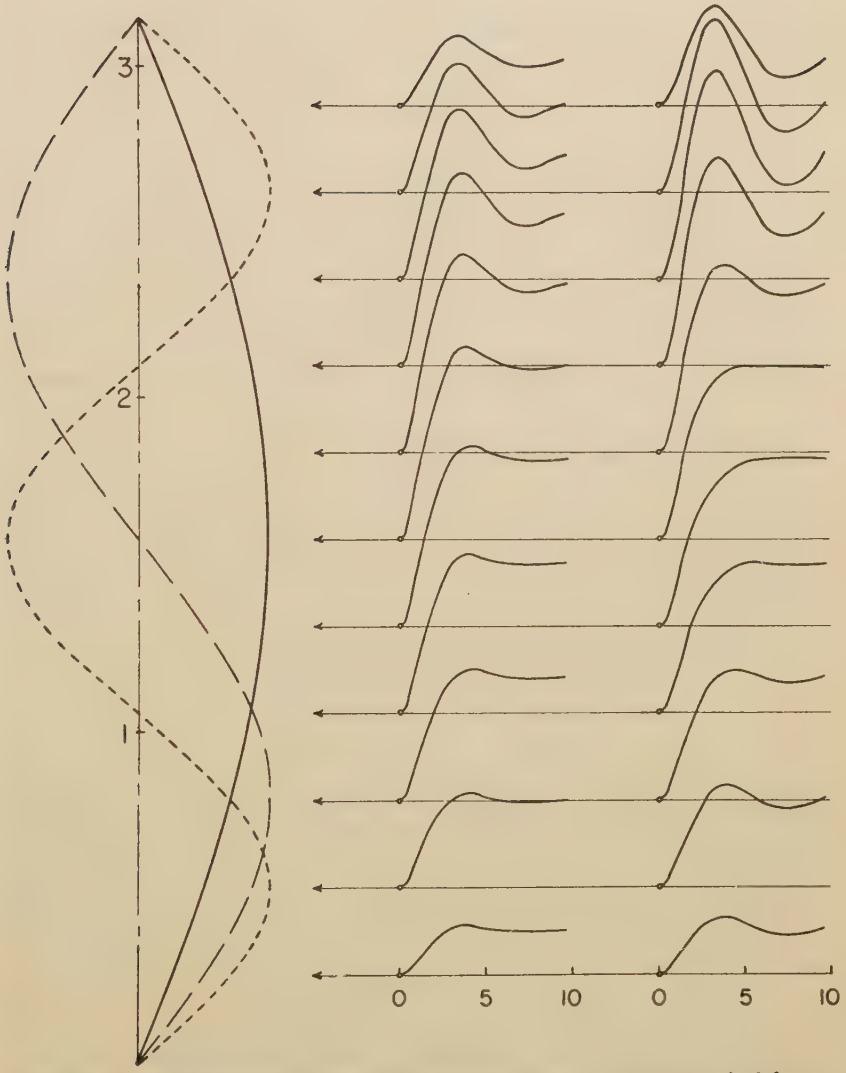

Figure 4. Profiles across Gulf Stream at various latitudes. The curves to the left represent sin y'', sin $2y''$, and sin $3y''$ as functions of y'', from $y'' = 0$ (15° N) to $y'' = \pi$ (50° N). The two columns to the right represent ψ' as function of x' at the latitudes indicated by the arrows, for $\lambda = 0.2$ (left) and $\lambda = 0.4$ (right). Unit values of ψ' correspond to twice the vertical distance between arrows.

where H is the thermocline depth in cm. Assuming a thermocline depth of 70 meters gives roughly $\lambda = 0.4$. Fig. 3 has been drawn for this value. The main current reaches its greatest intensity along $y'' = 0.7\pi$ instead of $y'' = 0.5\pi$. This represents a displacement northward by 7° latitude. Fig. 4 shows the combined profiles at various latitudes, for $\lambda = 0.2$ and $\lambda = 0.4$.

The general orientation of the Atlantic coastline differs markedly from the assumed north-south direction. The effect of the inclination of the coastline is to distort the circulation pattern and widen and weaken the current by a factor $(\sec\theta)^{1/3}$, as had already been pointed out by Munk and Carrier (1950). The relative effect of the higher order terms diminishes with the inclination of the coastline (equation 29), since the value of λ is to be multiplied by $\sqrt{p}$ or $(\cos\theta)^{2/3}$. For $\theta = 50°$, this amounts to 0.74.

THE CASE OF A VARIABLE THERMOCLINE DEPTH

We have assumed λ, and hence the depth of the thermocline, to be constant. Actually λ is considerably larger near shore, where the thermocline is shallow, than it is further offshore. This variation of thermocline depth *across* the current forms a vital part in Rossby's discussion.

To estimate the importance of this variation, set

$$H = \frac{H_0}{1 - \alpha\psi'}, \qquad \lambda_0 = \frac{29n^4\gamma\Gamma c}{400\bar{\rho}\beta^2\gamma^2 H_0}, \tag{31}$$

where H_0 is now the thermocline depth at the boundary. H will thus increase with distance from shore, reaching a value $H_0/(1 - \alpha)$ where ψ' becomes unity (Fig. 7).

Combining (31) with (6) and (8) gives

$$\left(\nabla'^4 - \frac{\partial}{\partial x'}\right)\psi' = \frac{1}{r'}\sin y'' + 4\gamma^{-1}\lambda_0(1 - \alpha\psi')\,\mathrm{curl}_z\,(\boldsymbol{M}' \cdot \nabla'\boldsymbol{M}') \tag{11v}$$

in place of equation (11). Carrying out solutions of this equation to only zero and first orders leads to equation (11.0) as before, and adds a new term

$$-2\alpha X_0 F_1 \sin y'' \sin 2y''$$

to equation (11.1). The particular and homogeneous integrals corresponding to $X_0F_1 \sin y'' \sin 2y''$ are

$$\left.\begin{aligned}\psi_v'^p = \Big[&-\frac{5}{6}e^{-x'} - \frac{i\sqrt{3}\omega}{9}x'e^{\omega^2 x'} + \frac{i\sqrt{3}\omega^2}{9}x'e^{\omega x'} + \frac{1}{42}e^{2\omega^2 x'} \\ &+ \frac{1}{42}e^{2\omega x'} - \frac{i\sqrt{3}}{126}(5+\omega)\,e^{(\omega^2-1)x'} \\ &+ \frac{i\sqrt{3}}{126}(5+\omega^2)\,e^{(\omega-1)x'}\Big]\sin y''\sin 2y'' ,\end{aligned}\right\} \quad (20v)$$

$$\psi_v'^h = [a_v e^{\omega^2 x'} + \bar{a}_v e^{\omega x'}]\sin y''\sin 2y'' , \quad (21v)$$

where

$$a_v = \frac{8}{21} - \frac{25i\sqrt{3}}{126} ,$$

and $\bar{a}_v$ is its conjugate. The complete solution of the zero and first order is then

$$\psi' = X_0 \sin y'' + \lambda_0 (X_1 \sin 2y'' - 2\alpha X_v \sin y'' \sin 2y'') , \quad (22v)$$

where

$$\begin{aligned}X_v = \Big[&-\frac{5}{6} + \frac{1}{21}\cos\sqrt{3}x'\Big]e^{-x'} + \Big[\Big(\frac{x'}{3} + \frac{16}{21}\Big)\cos\frac{\sqrt{3}x'}{2} \\ &+ \Big(\frac{\sqrt{3}x'}{9} - \frac{25\sqrt{3}}{63}\Big)\sin\frac{\sqrt{3}x'}{2}\Big]e^{-\frac{x'}{2}} + \Big[\frac{1}{42}\cos\frac{\sqrt{3}x'}{2} \\ &- \frac{\sqrt{3}}{14}\sin\frac{\sqrt{3}x'}{2}\Big]e^{-\frac{3}{2}x'} \quad (23v)\end{aligned}$$

has been plotted in Fig. 5. The function is very similar to X_1, and the two first order solutions cancel to a large degree. Fig. 6 shows the streamlines according to (22v) for $\alpha = 0.75$, $\lambda_0 = 0.6$. Except for a slight tendency for the north-flowing current to "overshoot," there is little deviation from the zero order solution.

It must be emphasized that the results depend somewhat on our choice of the numerical constants and on the rather arbitrary form of equation (31). This description of the variation in thermocline depth was chosen for its suitability in the computation of higher order terms. Actually our model for the density structure, when combined with the geostrophic equations for the currents, completely specifies the law for the variation in thermocline depth, but the resulting expression is not suitable for the computation of higher order terms (see Fig. 7).

Let us define a stream function ϕ, related to the surface mass trans-

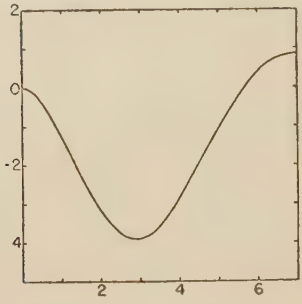

Figure 5. The function X_v (Equation 23v) associated with a variable depth in thermocline.

port $\rho_0 \mathbf{v}_0$ in the same manner as ψ is related to the integrated transport. Then the geostrophic equations, with the aid of (2) and (3), can be written

$$f\nabla\phi = \nabla p_0 = \rho_0 g \nabla h ,$$

$$f\nabla\psi = \int_{-\infty}^{h} \nabla p dz = \frac{5\rho_0^2 g}{8\Delta\rho} \nabla h^2 .$$

Solving for h, and neglecting the variation with latitude of the Coriolis' parameter f, leads to

$$h = \frac{f}{\rho_0 g}\phi + h_0 = \sqrt{\frac{8f\Delta\rho}{5\rho_0^2 g}\psi + h_0^2} ,$$

where h_0 is the value of h for $\theta = \psi = 0$. It follows from (1) that $H_0 = h_0\rho_0/2\Delta\rho$ is the depth of the thermocline at the boundary. The above equations can be solved to yield

$$\phi = \frac{\sqrt{1 + a\psi} - 1}{\frac{5}{4}aH_0}, \qquad H = H_0\sqrt{1 + a\psi} , \qquad (32a, b)$$

where

$$a = \frac{2f}{5g\Delta\rho H_0^2} .$$

In order for (31) to be a suitable approximation to (32b), it would be necessary that $a\psi' << 1$ and $a\psi << 1$. Actually $a\psi$ varies from zero to fourteen.

For a numerical example we choose conditions at $y'' = \pi/2$, the approximate latitude of Cape Hatteras. Setting $f = 10^{-4}$ sec^{-1}, $g =$

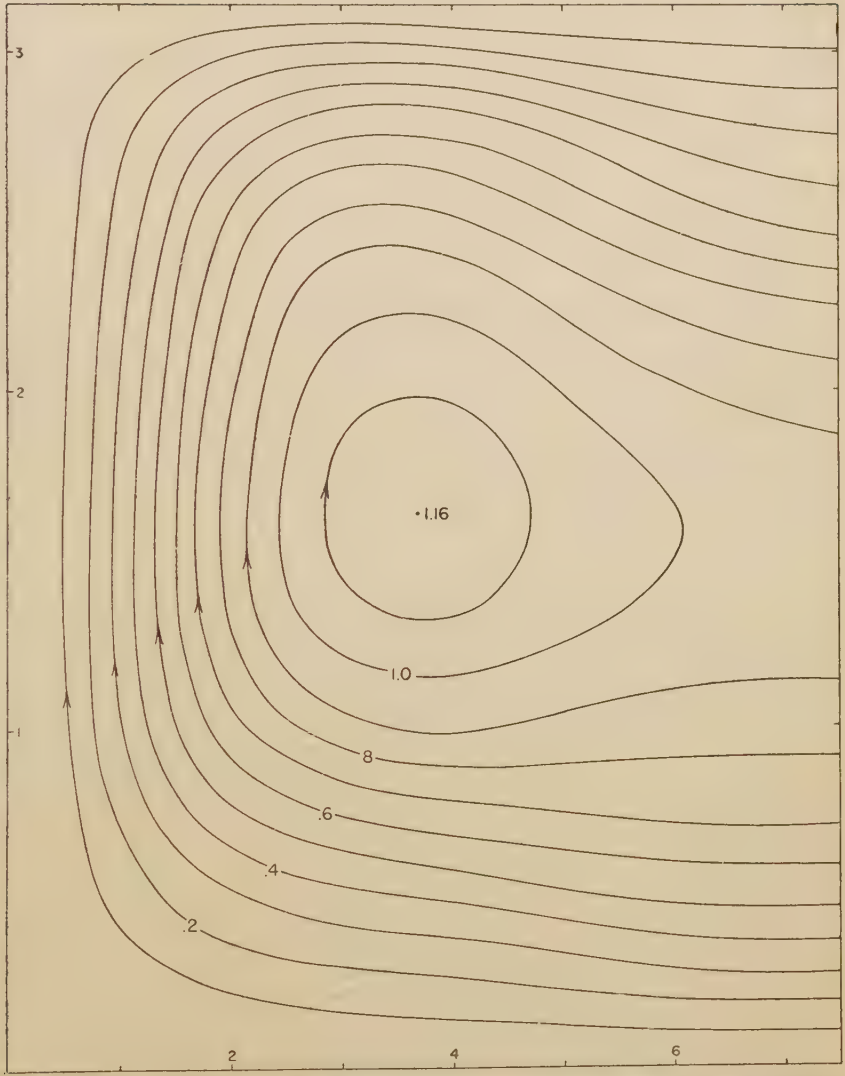

Figure 6. Streamlines of mass transport, ψ', for the combined zero and first order solutions pertaining to a variable depth in thermocline (Equation 22v), assuming $\alpha = 0.75$. The corresponding profile of the thermocline is presented by the dashed curve in the lower portion of Fig. 7.

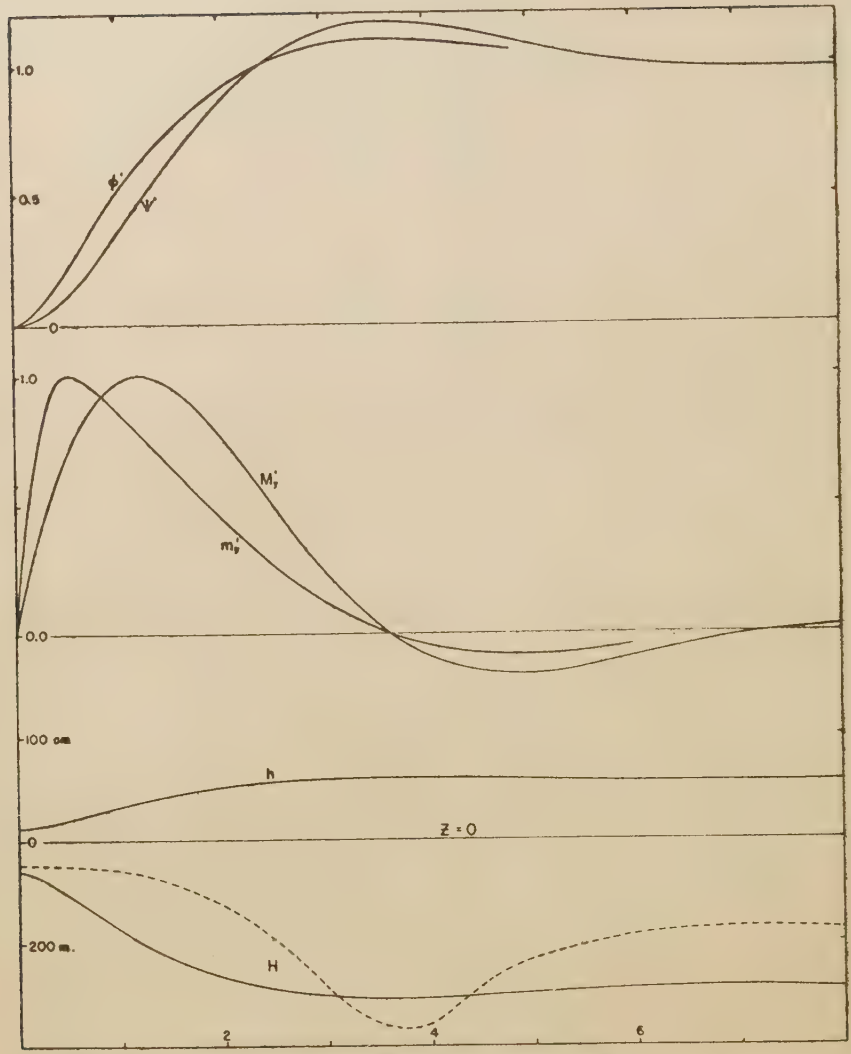

Figure 7. Variation of parameters across the Gulf Stream according to the zero order solution. A unit distance x' equals approximately 50 km. The upper curves denote the surface stream function ϕ' and integrated stream function ψ'. For $\phi' = 1$, $\phi = 4.51 \times 10^8$ g sec^{-1} cm^{-1}; $\psi' = 1$, $\psi = 1.95 \times 10^{13}$ g sec^{-1}. The central curves show the corresponding surface transports and integrated transports. For $m_y' = 1$, $m_y = 55.3$ g sec^{-1} cm^{-3}; $M_y' = 1$; $M_y = 2.13 \times 10^6$ g sec^{-1} cm^{-1}. The lower solid curves represent the surface and thermocline profile according to Equation (32v). The dashed curve is the assumed thermocline according to (31).

10^3 g sec^{-2}, $\Delta\rho = 10^{-3}$ g cm^{-3}, $H_0 = 6000$ cm, gives $a = 1.11 \times 10^{-12}$ g^{-1} sec. Furthermore nr $= 6$, $\Gamma = 0.65$ dynes cm^{-2}, $\beta = 2 \times 10^{-13}$ cm^{-1} sec^{-1}. The lower portion of Fig. 7 shows the surface profile and thermocline profile according to equations (1) and (32b). For comparison we have added the thermocline according to (31), assuming that the depth at the boundary is 4,640 cm, which gives the value of 0.6 from equation (30).

The upper curves show the zero solution for ψ' (equation 15) and the corresponding surface stream function according to (32a). The central curves represent the slopes of the upper curves and are proportional to surface current and integrated current, respectively. The distance between maximum current and the left edge is about 25 km at the surface and 60 km for the integrated current. The reason for the displacement of the maximum in the surface current has to do with the variation of the vertical structure across the stream. At the left side (looking downstream) the current is superficial and the surface velocities large. Towards the right the current extends to greater depth, and the surface velocities are relatively small.

CONCLUSIONS

The westward intensification according to the planetary vorticity theory is therefore even more pronounced if surface currents are considered rather than the integrated transport. The width of 25 km for the "cold wall," which corresponds to a value of $A = 2.5 \times 10^7$ cm^2 sec^{-1}, $p = 0.445$ (Munk and Carrier, 1950: fig. 4), is in agreement with observations in the Hatteras area.

Our examination is unrealistic for a number of reasons. We have assumed the western boundary to be a vertical wall. The bottom rises gradually, of course, and many of the modifications inshore of the Gulf Stream take place over the Continental Shelf. We have also neglected the effect of the indentations in the coastline. Furthermore, the eddy viscosity is taken as constant, whereas in Rossby's theory this coefficient varies along the Stream. Our zero order solution, as represented by the central curves in Fig. 7, resembles the wake stream profile (Rossby, 1936: fig. 4). However, this resemblance is not noticeably improved by the inclusion of higher order terms.

At the outset of this investigation it was hoped that the higher order terms might contain a clue as to the continued concentration of the Gulf Stream long after it has left the American east coast. Another observed feature not contained in the linear solution is the countercurrent inshore (Bumpus and Wehe, 1949). Even though the validity of the higher order terms is in doubt, largely because of their

surprisingly strong dependence on the assumed vertical distribution of density, it does not seem likely that these observed features are contained in the higher order terms. There is some essential feature in the dynamics (or thermodynamics) of the Gulf Stream which has not yet been recognized.

REFERENCES

Bumpus, D. D. and T. J. Wehe
1949. Hydrography of the western Atlantic; Coastal water circulation off the east coast of the United States between Cape Hatteras and Florida. Tech. Rep. Woods Hole Oceanogr. Instn., 16.

Iselin, C. O'D. and F. C. Fuglister
1948. Some recent developments in the study of the Gulf Stream. J. Mar. Res., *7:* 317–329.

Munk, W. H.
1950. On the wind-driven ocean circulation. J. Meteorology, *7(2):* 79–93.

Munk, W. H. and G. F. Carrier
1950. The wind-driven circulation in ocean basins of various shapes. Tellus (in press).

Reid, R. O.
1948. A model of the vertical structure of mass in equatorial wind-driven currents of a baroclinic ocean. J. Mar. Res., *7:* 304–312.

Rossby, C. -G.
1936. Dynamics of steady ocean currents in the light of experimental fluid mechanics. Pap. phys. Oceanogr., *5 (1):* 43 pp.

Stommel, Henry
1948. The westward intensification of wind-driven ocean currents. Trans. Amer. geophys. Un., *29:* 202–206.

Von Arx, W. S.
1950. An electrical method for measuring the velocity of ocean currents from a ship underway. Pap. phys. Oceanogr., *11 (3).*

NOTE TO AUTHORS

The pages of this Journal are open to all contributors, and manuscripts may be submitted to any member of the Board of Editors or to the Managing Editor. Publication will be made only in the English language, but copy may be submitted for consideration in other languages. Aid in translation of accepted manuscripts will be given when possible.

All manuscripts should be typewritten with double space, carefully corrected, with footnotes continuously numbered and set off in the body of the text. If an article is to appear as a contribution from another institution, it should be approved by that institution before submission; contribution numbers of such institutions are submitted with the return of galley proofs.

The author (or authors) of each article will receive a total of 50 free reprints (with covers). Additional reprints with or without covers may be ordered by authors or institutions at the cost of printing. Orders for reprints are given when galley proofs are returned.

Both galley and page proofs are submitted to the senior author of each article.

Tables should be prepared for clarity and as near as practicable to Journal pattern, without ruled lines if possible. Table footnotes should appear at the base of each Table.

Figures are required for consideration simultaneously with the manuscript. Original figures of inconvenient size for forwarding may be represented by photographs on first submission of a manuscript; originals are required for line cuts. Illustrations requiring half-tone reproduction should be avoided as far as possible, but they will be accepted when necessary. *It is very important that the proper size of characters and symbols should be used for the lettering of illustrations.* A diagram for determining suitable heights of letters for original drawings that will be reduced, together with an explanatory note, has been published in this Journal, Vol. III, No. 1: 89–91; reprints will be submitted to authors on request. Mechanical lettering is recommended. If facilities for lettering are not available to the author, it is preferable to receive illustrations with lettering indicated in pencil only, to be finished in ink in the editorial office. All illustrations will be subject to at least a minimum reduction at the rate of 1 : 1.2. Drawings which have been heavily patched and pasted must *not be rolled* for mailing. The legends for the figures, identified by corresponding figure numbers on the illustrations also, should be typed in sequence at the end of the manuscript.

A complete and *accurate list of references* in alphabetical order at the end of each article is essential. References may be indicated in the text by author's name (or names) and *year of publication*, or by italicized numbers which correspond to the numbers given in sequence in the list of references. Each reference should include the last name followed by at least two initials or first name; co-authors should be listed with the initials or first name preceding the last name. The date should be indented on the line below, followed by a complete title *verbatim* in lower case except for the first word. Publisher, city and pagination should be indicated for books; for periodicals (abbreviations from "World List of Scientific Periodicals," Oxford, as far as possible), the volume (italicized), number and pagination should be given.

Additional information regarding the preparation of manuscripts will be furnished by the Managing Editor.

TABLE OF CONTENTS

Page

1. **Gifford Ewing**: Slicks, surface films and internal waves..... 161

2. **W. R. Coe and John E. Fitch**: Population studies, local growth rates and reproduction of the Pismo clam (*Tivela stultorum*).... 188

3. **G. J. Lewis with T. G. Thompson**: The effect of freezing on the sulfate/chlorinity ratio of sea water..... 211

4. **W. H. Munk, G. W. Groves and G. F. Carrier**: Note on the dynamics of the Gulf Stream..... 218

NOTICE

The PREVENTION OF DETERIORATION ABSTRACTS, published by the National Research Council (Prevention of Deterioration Center, Room 204), 2101 Constitution Avenue, Washington 25, D. C., are offered for subscription on a yearly basis. Abstracts are classified under the headings: Biological agents; Electrical and electronic equipment; Fungicides and other toxic compounds; Lacquers, paints, and varnishes; Leather; Lubricants; Metals; Miscellaneous; Optical instruments and photographic equipment; Packaging and storage; Plastics, resins, rubbers, and waxes; Textiles and cordage; and Wood and paper. One volume of approximately 2000 loose-leaf pages is published each year in monthly issues. Subject and author indexes are compiled annually to cover abstracts issued from July through June. The yearly rate of $50.00 includes two sturdy binders and index tabs.

An ADVANCE LIST, a monthly bibliography of all reports received in this field, is available for $10.00 a year.